Research Article

Received: 12 September 2025 Revised: 21 April 2026 Published online in Wiley Online Library:

(wileyonlinelibrary.com) DOI 10.1002/ps.70952

Integrating habitat suitability, socioeconomics, and infrastructure to assess global biological invasion risk under climate change: A case study of the rice stem borer, *Chilo suppressalis*

Jinsol Hong,[a] Minyoung Lee,[b,c] Yongeun Kim,[a] Yun-Sik Lee,[d] June Wee,[e] Jaejun Song,[a] Taewoo Kim,[f] Jung-Joon Park,[g] Florian Kraxner,[h] Woo-Kyun Lee,[a,f] Youngil Song[i] and Kijong Cho[a,f*]

Abstract

BACKGROUND: Biological invasion risk is a multifaceted concept that, according to the Food and Agriculture Organization (FAO), results from the likelihood of entry, establishment, and dispersal, along with the potential impact magnitude. Based on this definition, we developed a national-scale risk index using normalization and entropy-based objective weights. The striped rice stem borer (RSB, *Chilo suppressalis*) was used as a case study to demonstrate global invasion risk under Shared Socioeconomic Pathway (SSP) scenarios. Our framework integrated key data, including trade volume, transportation networks, cropland cover, irrigation, the Ecoclimate Index (EI) from the CLIMEX model, and rice harvest area to construct likelihood, and magnitude criteria. The final risk index (Risk) was calculated by multiplying likelihood and magnitude.

RESULTS: Substantial inhabitable areas (EI > 0) exist in Africa (60.7% of land area), North America (36.1%), and South America (85.6%). Risk was highest in South America (0.21), followed by Africa (0.18), North America (0.17), and Europe (0.08). Under SSPs, climate and land cover changes are projected to intensify regional differences in invasion risk. Risk is expected to increase in South America under all SSPs and in Europe under SSP585. In contrast, Risk is projected to decline in North America under all SSPs, while in Africa it shows a slight increase around the 2050s before decreasing.

CONCLUSION: RSB has sufficient potential to threaten global food security. Given the varied regional patterns of risk components, proactive, region-specific biosecurity measures are essential for high-risk hotspots. The proposed framework provides a valuable tool for pest risk assessment.

* *Correspondence to: K Cho, Ojeong Resilience Institute, Korea University, Seoul, 02841, Republic of Korea. E-mail: kjcho@korea.ac.kr*

a *Ojeong Resilience Institute, Korea University, Seoul, Republic of Korea*

b *Department of Integrative Biology, Michigan State University, East Lansing, USA*

c *Ecology, Evolution, and Behavior program, Michigan State University, East Lansing, USA*

d *Department of Biology Education, Pusan National University, Busan, Republic of Korea*

e *Department of Applied Biology, Chungnam National University, Daejeon, Republic of Korea*

f *Department of Environmental Science and Ecological Engineering, Korea University, Seoul, Republic of Korea*

g *Department of Plant Medicine, Gyeongsang National University, Jinju, Republic of Korea*

h *Agriculture Forestry and Ecosystem Services Group, Biodiversity and Natural Resources Program, International Institute for Applied Systems Analysis (IIASA), Laxenburg, Austria*

i *Korea Adaptation Center for Climate Change, Korea Environment Institute, Sejong, Republic of Korea*

Supporting information may be found in the online version of this article.

Keywords: climate change; entropy weight method; invasive species; pest risk assessment; rice stem borer (*Chilo suppressalis*); shared socioeconomic pathways (SSPs)

1 INTRODUCTION

Invasive species pose a significant threat to the global environment, causing severe ecological, economic, public health, and cultural impacts.[1–3] The rapid growth of global trade and transportation has intensified the risk of biological invasions, as increasing mobility through traded goods and efficient intercontinental transport networks enables species to overcome climatic and geographical barriers. According to the World Trade Organization, global trade volume increased by more than 4500% between 1950 and 2024.[4]

The introduction of invasive insects into previously inaccessible regions has resulted in major ecological disturbances and economic losses. Over the past five decades, the annual global economic cost of invasive species has exceeded $1.3 trillion,[5] with invasive insects alone responsible for at least $70.0 billion per year.[6] Despite broad consensus on the need for targeted management to mitigate impacts and prevent introductions, significant challenges remain. Proactive identification of potential risk hotspots is therefore essential for effective management strategies.[7]

Climate change further complicates invasive insect management by altering potential invasion areas as historically limiting climatic barriers weaken.[8] When a species arrives in a location newly suitable under climate change, whether deliberately or accidentally introduced, its population dynamics may deviate from those in its native range.[9] These flexibilities can lead to unexpected distribution patterns and impacts. Thus, adaptive pest management strategies that account for escalating invasion risks under future climates are imperative. To predict the geographic distribution of invasive species under climate change, Species Distribution Models (SDMs) have been widely applied.[10] SDMs can be useful tools for understanding ecological dynamics in novel habitats.[11] Their outputs are typically interpreted as indicators of potential distribution, habitat suitability, or invasion risk.[12,13] However, SDMs only assess invasion risk in terms of environmental suitability for establishment.[11,14]

As invasion risk is determined by multiple components, it cannot be defined solely by habitat suitability changes predicted by SDMs. The relative importance of these components depends on species ecology, trade and transport connectivity, and the ecological and agroeconomic context of recipient regions.[15] These complexities highlight the need for integrated frameworks that consider both biophysical and socioeconomic dimensions of invasion dynamics. Yet, research adopting this comprehensive approach remains limited. According to the Food and Agriculture Organization's pest risk analysis framework,[16] invasion risk encompasses the likelihood of entry, establishment, spread, and impact (Fig. 1). Entry indicates the likelihood of a pest entering the target area through human-mediated or natural pathways. Establishment denotes the probability of survival and reproduction after entry. Dispersal refers to spread from the initial establishment site to other areas. Magnitude was defined as the pest's potential economic significance, including direct and indirect damage and expected control costs.[16] Effective invasive species management therefore requires detailed understanding of the invasion process.[17]

This study addresses that gap by focusing on the striped rice stem borer (RSB, *Chilo suppressalis*), a major rice pest in Asia and Oceania.[18,19] RSB has limited dispersal capacity, with adults typically moving only 1–3 km.[20] Its long-distance spread is therefore linked primarily to rice trade. Newly hatched larvae bore into stems, producing 'dead hearts' or 'white heads,' which can reduce yields by up to 60%.[21] After harvest, larvae overwinter in straw and stubble, facilitating spread through trade in rice straw and related products. RSB originated in tropical and temperate Asia and Oceania.[18,19] Compared with other *Chilo* species, it shows greater cold tolerance, extending to the Russian Far East.[22] During the 20th century, RSB spread globally from its native range. It invaded Hawaii in the late 1920s *via* rice straw packaging, causing such severe damage that some farmers abandoned rice cultivation.[23,24] It became a serious pest in Spain after 1933[25,26] and expanded into Iran and Russia's Astrakhan region in the 1970s.[27,28] Although absent from the Americas and Africa, the expansion of rice cultivation in these regions raises concern over its potential invasion, particularly under climate change.

This study aims to develop a novel invasion risk assessment framework applicable to regions where RSB is not yet present. This framework is built based on CLIMEX, one of the most widely used semi-mechanistic SDM,[29] and integrates key invasion risk factors. CLIMEX is widely used to assess the invasion risk of poikilothermic species under novel climate conditions.[30] It assumes that climatic factors primarily constrain species distributions and score the ecoclimatic suitability of each grid cell based on biophysical parameters of the target species.[29] Due to this fundamental assumption of the model, CLIMEX alone cannot fully capture invasion risk. Therefore, we embedded CLIMEX-based climatic suitability within a broader invasion risk assessment framework that explicitly incorporates these additional factors. Specifically, we aim to: (i) model the global potential distribution of RSB using CLIMEX; (ii) project distribution changes under climate and land cover scenarios; and (iii) develop and evaluate a composite invasion risk index that incorporates critical factors in RSB invasion process.

2 MATERIALS AND METHODS

2.1 Concept of invasion risk, and its components

The FAO[16] proposed a framework for assessing invasion risk in quarantine pests. In this framework, invasion risk (Risk) is determined by both the likelihood of invasion (Likelihood) and the potential magnitude of impact (Magnitude). The risk formula was expressed as follows:

$$Risk = Likelihood \times Magnitude \quad (1)$$

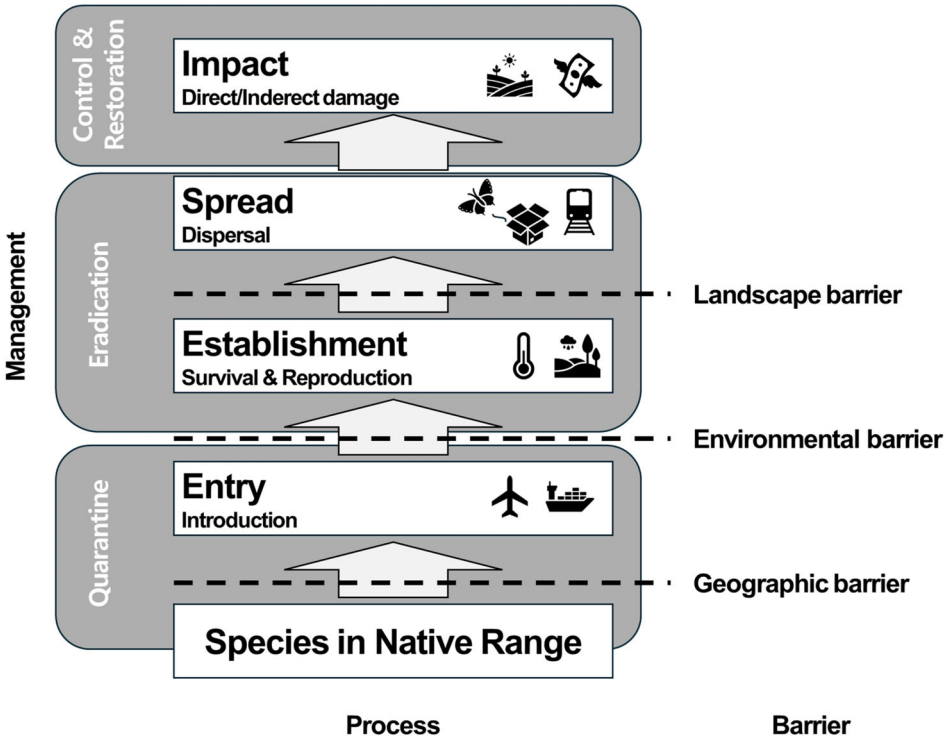

Figure 1. Process of biological invasion, major barriers at each stage, and corresponding management actions.

Figure 2 illustrates the overall structure of the invasion risk assessment framework used in this study. In brief, the framework is designed to systematically integrate climatic suitability with the anthropogenic and landscape drivers that govern the risk of RSB invasion at a national scale. Key indicators for each criterion were derived from data sources to comprehensively assess RSB invasion risk (Table 1). Entry and Dispersal were assumed to depend on trade, transportation, and local infrastructure, while Establishment was linked to habitat suitability under climate change.

2.2 Current RSB occurrence data

RSB occurrence records were compiled from multiple sources, including online databases (GBIF and iNaturalist), academic literature, and the Center for Agriculture and Bioscience International[22,39] (Fig. 3; Supplementary 1). For studies providing GPS coordinates, data were used directly. Where only locality names or map figures were available, geocoding was performed using Google Maps. Duplicate and erroneous records were removed, and observations were filtered to ensure one record per 10′ grid cell. The final dataset contained 342 distinct occurrence records. RSB is currently distributed across South Asia, Southeast Asia, East Asia, Oceania, the Pacific Islands, and parts of Europe, with no reports in the Americas or Africa.[21,22]

2.3 Future scenarios: shared socioeconomic pathways (SSPs)

Future projections incorporated both climate and land cover using four standard Shared Socioeconomic Pathways (SSPs): SSP126, SSP245, SSP370, and SSP585.[40,41] The first digit represents a socioeconomic pathway, and the last two digits indicate projected radiative forcing by anthropogenic greenhouse gases in 2100 (W m^{-2}). SSP585 reflects the most extreme climate change scenario, while SSP370 projects the largest cropland expansion due to population growth and limited trade.[36] These scenarios represent varying levels of global mitigation and adaptation efforts (Supplementary 2).

2.3.1 *Climatic variables*

Current climate conditions were represented using CliMond 10′ gridded global data (CM10_1975H_v1.2.mm), covering the 1961–1990 baseline.[42] Future climate projections under each SSP were obtained from the CNRM-CM6-1-HR model (CMIP6) *via* the Earth System Grid Federation (ESGF).[43,44] This high-resolution model (50 km) enabled detailed global projections. Future projections are targeted at 2050s (mean of 2036–2065) and 2080s (mean of 2066–2095) for each scenario.

CLIMEX requires monthly maximum and minimum temperatures, precipitation, and relative humidity (RH) at 9:00 and 15:00 h.[29] Since the CNRM-CM6-1-HR does not provide RH at these times, values were estimated using the method of Kriticos *et al.*[42]

2.3.2 *Land cover*

Since CLIMEX relies solely on climatic variables, land cover data was used exclusively for deriving indicators within the invasion risk assessment framework. Future land cover scenarios were obtained from Chen *et al.*,[36] who generated a global 1-km projection of seven land types—forest, grassland, barren, cropland, urban, water, and permanent snow/ice—using the artificial neural network-based GeoSOS-FLUS v2.4 model, driven by CMIP6 Land-Use Harmonization 2. This dataset provides dynamic land cover changes at 5-year intervals from 2015 to 2100. Accordingly, land covers for 2050s and 2080s were represented using the 2050 and 2080 data for each SSP.

Since RSB primarily occurs in cultivated areas,[22] our analysis focused on cropland grids derived from the land cover layers to

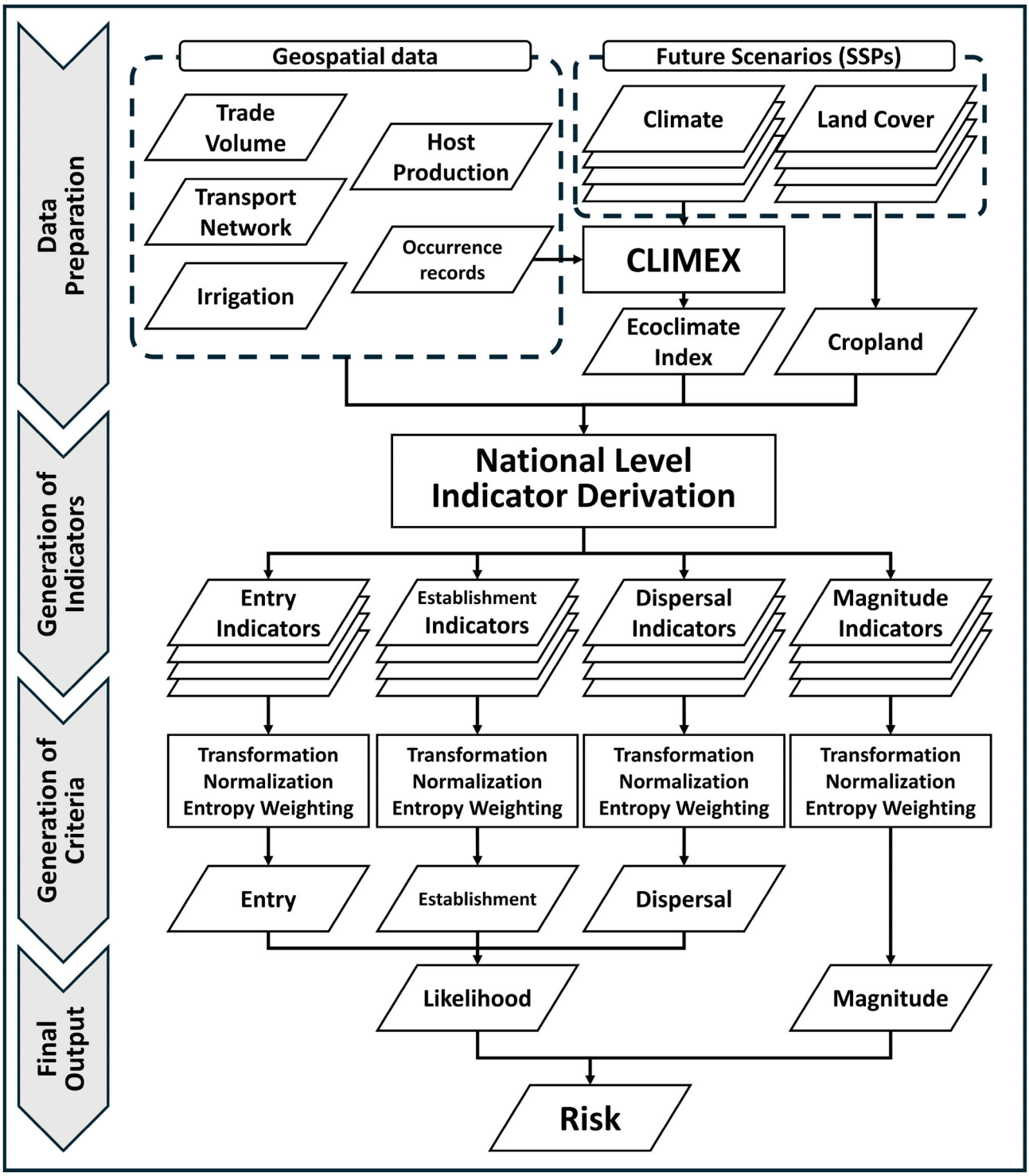

Figure 2. Schematic flowchart for the invasion risk assessment framework.

generate cropland-based indicators related to host availability and establishment potential. Since rice harvest area projections under SSPs are unavailable, we assumed that the proportion of rice area in each country, derived from the CROPGRID v1.08 dataset,[38] would remain constant. Thus, we estimated prospective rice harvest areas by applying this ratio to projected changes in cropland under each SSP.

2.4 Indicators for the likelihood criterion

2.4.1 Entry

This sub-criterion represents the likelihood that RSB will enter a given country. In this study, the likelihood of Entry was estimated using three groups of indicators: (i) global trade volume, (ii) transport connectivity, and (iii) geographic distance from countries where RSB is present (see Table 1). This conceptualization followed the pest risk

Table 1. Selected indicators for assessing the invasion risk of *Chilo suppressalis* for each country

Criterion		Indicators	Description	Unit	SSP*	Source
Likelihood	Entry	$CARGO_{total}$	20-year (from 2000 to 2019) import quantity of 'Cereal straw and husks (World Customs Organization Harmonized System item code: 121300)'.	kg	-	31
		$CARGO_{rsb}$	Subset of $CARGO_{total}$, including only countries where *C. suppressalis* is currently present.	kg	-	31
		$PORT_{water}$	Number of entry water ports by each country.	No.	-	32
		$PORT_{air}$	Number of international airports by each country.	No.	-	33
		$CROSS_{road}$	Number of roads that cross the border.	No.	-	34
		$CROSS_{rail}$	Number of railways that cross the border.	No.	-	35
		PROX**	Relative geographic distance from the closest country where *C suppressalis* currently occurs is explicitly categorized as follows. 1.0: Countries that share a land border with a country where *C. suppressalis* is currently present. 0.75: Countries located on the Eurasian mainland but do not directly share a border. 0.5: Island countries in Asia and Europe, countries in Oceania, and countries in Northern Africa. 0.25: Sub-Saharan African countries. 0.0: Countries in the Americas.	-	-	This study
	Establishment	EI_{port}	Mean of EI*** at all ports.	-	C	This study
		$EI_{cropland}$	Mean of EI at croplands.	-	C/L	This study
		$AREA_{EI9.58}$	Area of cropland where EI > 9.58****.	ha	C/L	36
		$AREA_{irrig}$	Area of irrigation in the cropland.	ha	L	37
	Dispersal	$DIST_{port}$	Mean distance of croplands from ports (water + air).	km	L	32,33
		$DENS_{road}$	Density of roads in croplands.	m km^{-2}	L	34
		$LENG_{rail}$	Total length of railway.	km	-	35
Magnitude		$AREA_{rice}$	Harvest area for rice production by each country.	ha	L	38
		$PROP_{rice}$	Proportion of $AREA_{rice}$ over the total harvest area by each country.	0.01%	L	38

Note: *Indicates whether climate (C) or land cover (L) change affects the indicator under Shared Socioeconomic Pathway (SSP) scenarios. **Full list of countries for each class is provided in Supplementary 4. ***CLIMEX Ecoclimatic Index. ****Mean EI of RSB occurrences in Europe, applied as an empirical threshold to define the suitability margin of RSB invasion.

analysis guidance, which indicates that the probability of entry is shaped by the pathways linking source and destination areas, the volume and frequency of movement along those pathways, and the possibility of natural spread from areas where the pest is already present.[45] Although SSP scenarios could substantially influence future global trade and transport infrastructure, static datasets were used due to limited projections. The implications of this limitation are discussed in the *Discussion* section.

Our indicator selection for trade-related indicators followed two main considerations: (i) documented relevance to the biology of RSB, and (ii) availability of globally comparable data. Two indices were calculated for each country: the total quantity of items traded ($CARGO_{total}$) and the proportion of imports from countries where RSB is present ($CARGO_{rsb}$). The most relevant trade item is cereal straw, as the primary invasion pathway is hitchhiking via rice stubbles and straws.[22] Historical records also suggest that the introduction into Hawaii was associated with infested rice straw used as packing material.[24] Therefore, 20 years (2000–2019) of import data for 'Cereal straw and husks' (World Customs Organization Harmonized System code: 121300) were obtained from WITS (2023). The WITS database provides both total import volumes and country-specific volumes for each commodity. Using these data, we calculated the proportion of imports that originated from RSB-present countries.

Transport connectivity was measured by the number of potential entry points in each country: (i) water ports (rivers and seas[32]), (ii) airports,[33] (iii) roads,[34] and (iv) railways[35] (see Supplementary 3). For water ports, only officially designated entry ports were included ($PORT_{water}$); for airports, only international airports ($PORT_{air}$). For roads and railways, the number of border crossings with neighboring countries was counted ($CROSS_{road}$ and $CROSS_{rail}$). The $CROSS_{road}$ and $CROSS_{rail}$ indicators were applied only to countries on the Eurasian mainland.

Finally, an ordinal proxy indicator (PROX) was used to represent the likelihood of entry based on geographic proximity to the nearest RSB-present country. Because there are no globally available, standardized metrics that quantify natural dispersal-driven entry, we conceptualized this indicator to capture relative geographic connectivity. The index was categorized as follows:

- Class 1: Countries sharing a land border with an RSB-present country
- Class 2: Eurasian mainland countries without a direct border

Pest Management Science published by John Wiley & Sons Ltd on behalf of Society of Chemical Industry.

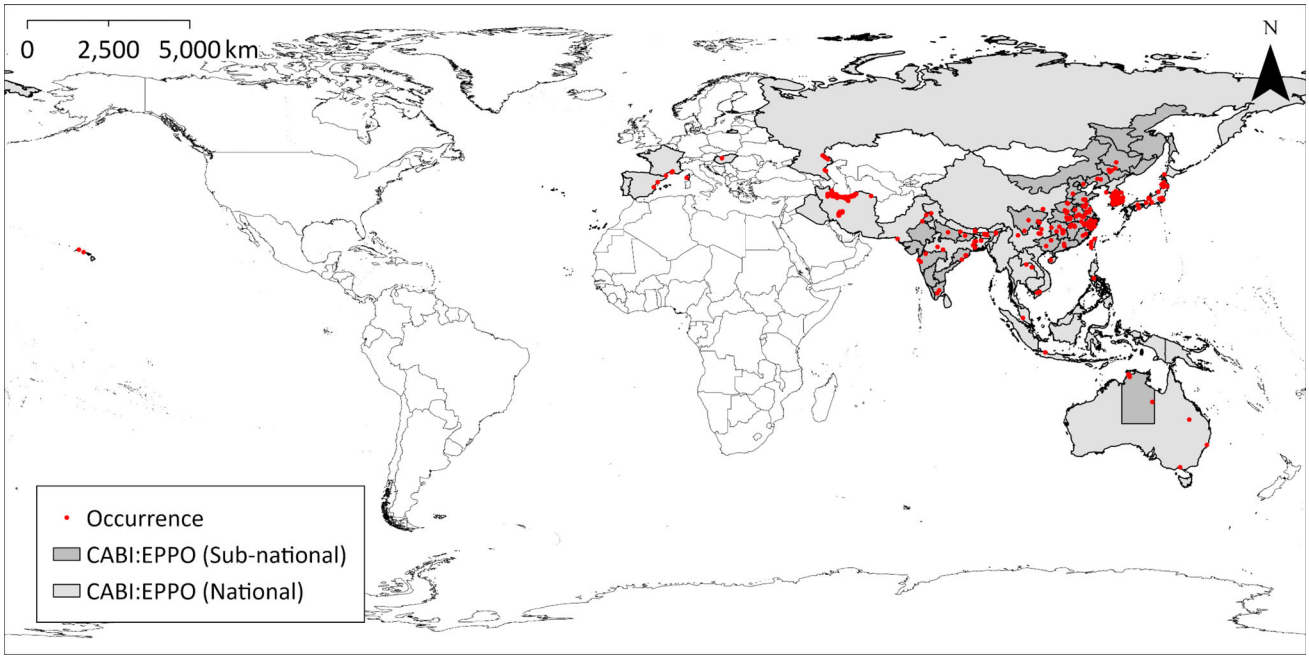

Figure 3. Current occurrences and distribution of *Chilo suppressalis*. Red dots indicate occurrence localities. National (light grey) and sub-national (dark grey) units reporting *C. suppressalis* are from CABI/EPPO.

- Class 3: Island countries in Asia/Europe, Oceania, and Northern Africa
- Class 4: Sub-Saharan African countries
- Class 5: Countries in the Americas

Each class was defined based on relative geographic proximity to countries where RSB is currently present, accounting for major geographic barriers such as oceans and deserts. We assigned values of 1, 0.75, 0.5, 0.25, and 0 to Classes 1–5, respectively, to represent a decreasing ordinal gradient of connectivity. Higher values indicate a greater likelihood of entry in terms of geographic connectivity rather than absolute distance. These values were evenly spaced to preserve the relative ordering of the classes. This classification quantifies the likelihood of RSB entry based on current distribution (Fig. 3). A full list of countries per class is provided in Supplementary 4.

2.4.2 *Establishment*

2.4.2.1. CLIMEX Model for RSB. This study employed the CLIMEX model (v4.0.2, Hearne Scientific Software, Australia) to project potential global establishment of RSB under current and future climates. The final output of CLIMEX is the Ecoclimatic Index (EI), ranging from 0 (unsuitable) to 100 (optimal year-round conditions).[29] EI is a composite of the Annual Growth Index (GI_A), representing population growth potential, and the Annual Stress Index (SI_A), quantifying climatic stress. Details are provided in Supplementary 5.

The development of the model began with a pilot model using parameter values from published literature and species' biophysical data ([18,46–52]). Then, the parameters were refined iteratively until the predictions aligned with the observed distribution (see Supplementary 6 for the detailed parameter fitting process). This study focused exclusively on calibrating the model to the native Asian range. European occurrences were retained as an independent reference for *post hoc* interpretation of EI. This approach was adopted to avoid potential circularity and ensure interpretative independence. The final parameter values are summarized in Table 2.

According to Kriticos *et al.*,[29] EI > 30 indicates suitability for at least one optimal growing season. In this study, the mean EI for all RSB occurrence points was 31.3, consistent with this threshold. However, no clear guidelines exist for finer suitability classes. To refine classification, Jenks's natural breaks optimization was applied to EI values for all inhabitable areas (EI > 0).[53] Breaks at EI = 13, 32, and 54 produced five categories: Uninhabitable (EI = 0), Marginal (EI = 1–13), Moderate (EI = 14–32), Favorable (EI = 33–54), and Very Favorable (EI = 55–100).

To further examine the response of the final model to climatic variables, a sensitivity analysis was performed using the built-in function in CLIMEX. Given that CLIMEX parameters operate on different scales, the default perturbation ranges were determined based on expert consensus.[29] The impact of each perturbation was evaluated by the percentage change in three categories: EI, Range, and Core Distribution. Parameters exerting a substantial effect on the model output were classified as 'sensitive' to the model, while those with no impact were deemed 'insensitive'. Specifically, Range represents grid cells where the EI value is greater than one. Core Distribution refers to the locations that are warm enough to complete at least one generation within a year while remaining free of stress indices.[29]

2.4.2.2. Indicators for establishment. Four indicators were developed from CLIMEX EI values to evaluate establishment potential (Table 1): (i) early establishment near major entry points (EI_{port}), (ii) climatic suitability of croplands ($EI_{cropland}$), (iii) total area of suitable croplands ($AREA_{EI9.58}$), and (iv) irrigation influence on establishment ($AREA_{irrig}$).

EI_{port}, derived from EI layers, assesses the likelihood of an initial population establishing near ports, the most probable entry points for RSB *via* trade. $EI_{cropland}$, the mean EI of croplands, was

Table 2. Final CLIMEX parameters for *Chilo suppressalis*

Category		Parameter	Description	Unit	Value
GI	TI	DV0	Lower temperature limit	°C	10
Growth	Temperature	DV1	Lower optimal temperature	°C	24
Index	Indices	DV2	Upper optimal temperature	°C	31
		DV3	Upper temperature limit	°C	36
		PDD	Degree-day for complete generation	DD[a]	840.34
	MI	SM0	Lower moisture limit		0.15
	Moisture	SM1	Lower optimal moisture		0.8
	Indices	SM2	Upper optimal moisture		2
		SM3	Upper moisture limit		2.5
SI	CS	TTCS	Cold stress temperature threshold (minimal temperature)	°C	−20
Stress	Cold Stress	THCS	Cold stress temperature rate (minimal temperature)	°C/week	−0.001
Index	HS	TTHS	Heat stress temperature threshold	°C	36
	Heat Stress	THHS	Heat stress temperature rate	°C/week	0.001
	DS	SMDS	Dry stress threshold	%	0.15
	Dry Stress	HDS	Dry stress rate	%/week	−0.005
	WS	SMWS	Wet stress threshold, wet stress begins to accumulate	%	2.5
	Wet Stress	HWS	When SM is above SMWS, wet stress accumulates	%/week	0.002

Note: Values without units represent dimensionless soil moisture indices (0 = over-dry, 1 = 100% moisture content capacity).
[a] Degree-day.

calculated by overlaying EI with land cover maps and reflects the overall climatic suitability of a country's croplands for RSB. The total cropland area with EI > 9.58 ($AREA_{EI9.58}$) was estimated by overlaying EI with SSP-specific land cover projections.[36] This threshold was based on the mean EI of 12 European sites where RSB has recently been established. Europe represents an active invasion front with climates distinct from its native Asian–Oceanian range, providing an appropriate benchmark for identifying marginal suitability and evaluating establishment potential in new environments. Using this empirically derived threshold enhances assessment realism by reflecting actual establishment conditions. Thus, this indicator comprehensively measures potential establishment areas by incorporating both climatic suitability and land use dynamics under current and future conditions. The irrigated cropland area ($AREA_{irrig}$) was estimated using three spatial datasets: actual irrigation area, percentage of area equipped for irrigation, and land cover.[36,37] This indicator is particularly relevant, as RSB thrives in humid environments and benefits from irrigation.

2.4.3 *Dispersal*

The likelihood of dispersal refers to the probability of spread from the initial introduction site to other areas. According to CABI,[22] local dispersal is mainly linked to host plant movement, particularly rice straw, as RSB adults and larvae disperse <3 km.[20]

Three spatial indicators quantified Dispersal: (i) average cropland distance from major ports and airports ($DIST_{port}$), reflecting natural or human-mediated dispersal from entry points; (ii) road density within croplands ($DENS_{road}$), indicating accessibility and potential for local dispersal via ground transport; and (iii) total railway length per country ($LENG_{rail}$), representing potential for long-distance overland dispersal.

Together, these indicators provide an integrated framework to assess RSB dispersal potential by combining transportation infrastructure and geographic context.

2.5 Indicators for the magnitude criterion

Magnitude encompasses both direct and indirect damage caused by the species, as well as the costs of control measures.[16,45] Since no global data are available on the Magnitude of RSB, this study assumed it is strongly correlated with rice production. Moreover, RSB invasion is expected to have greater significance in countries where rice is a key agricultural crop. The CROPGRID v1.08 dataset was used to generate magnitude indices.[38] This dataset contains crop area (physical area) and harvest area (sum of multiple harvests) for 173 crops across countries.

Two Magnitude indicators were developed: (i) the total harvested rice area in each country ($AREA_{rice}$), reflecting the absolute scale of potential agricultural losses due to RSB invasion; and (ii) the proportion of harvested rice area relative to the total national area ($PROP_{rice}$), representing the relative importance of rice cultivation and serving as a proxy for vulnerability to RSB impacts.

As no global projections of rice harvest area under future SSP scenarios are currently available, it was assumed that the proportion of rice harvest area within croplands would remain constant over time. Future rice harvest area was therefore estimated by applying this fixed proportion to the projected changes in cropland under each SSP land-use scenario.

2.6 Invasion risk assessment

A single integrated invasion risk index was derived for each country using a composite indicator model (Eqn (1)). This approach assumes all indicators in the model share the same unit.[54–56] Since this was not the case, each indicator was normalized to remove unit dependency, after which a set of weights was applied to the normalized indicators within each sub-criterion to calculate a single composite index.

2.6.1 *Data transformation and normalization*

All indicators in Table 1 were normalized using the widely applied min-max method.[54,55] First, the skewness of each indicator was

Pest Management Science published by John Wiley & Sons Ltd on behalf of Society of Chemical Industry.

assessed using the Fisher-Pearson method.[57] Indicators with skewness greater than |1| were Box-Cox power transformed prior to min–max normalization. Eqn (2) was applied to indicators positively associated with invasion risk, and Eqn (3) to those negatively associated[54]:

$$x_{is} = \frac{x_i - x_{imin}}{x_{imax} - x_{imin}} \quad (2)$$

$$x_{is} = \frac{x_{imax} - x_i}{x_{imax} - x_{imin}} \quad (3)$$

where x_i is the initial value of indicator i; x_{is} is the normalized value of indicator i; x_{imax} and x_{imin} are the maximum and the minimum values of x_i, respectively. After normalization, all indicators became dimensionless and ranged from 0 to 1.

2.6.2 *Entropy weighting method*

The relative importance of each criterion may vary regionally; however, determining universally applicable global weights is challenging. Therefore, each criterion was assumed to contribute equally to the overall risk assessment. To determine objective, data-driven weights for the indicators within each criterion, the entropy-based method of Zhu *et al.*[56] was applied as follows:

First, the global proportional matrix for each indicator i and country j (p_{ij}) was calculated using the normalized value x_{is}:

$$p_{ij} = \frac{x_{is}}{\sum_j^n x_{is}} \quad (4)$$

where x_{is} is the normalized value of indicator i for country j and n is the total number of countries. Since $\ln(0)$ is undefined, we set $p_{ij} \ln p_{ij}$ as 0 when $p_{ij} = 0$.[56]

Second, the global information entropy (E_i) of indicator i within each criterion was calculated as:

$$E_i = -\frac{\sum_{j=1}^n p_{ij} \cdot \ln p_{ij}}{\ln n} \quad (5)$$

E_i ranges from 0 to 1, with lower values indicating greater variability and higher discriminative power. The degree of diversification d_i was defined as:

$$d_i = 1 - E_i \quad (6)$$

A set of global weight (w_i) for each indicator was then determined by normalizing d_i:

$$w_i = \frac{d_i}{\sum_{i=1}^m d_i} \quad (7)$$

where m is the total number of indicators within the criterion. The sum of w_i values within each criterion equals 1. This method assigns greater weight to indicators with wider ranges, thereby increasing their contribution to the final index.

2.6.3 *Construction of likelihood and magnitude*

For countries where no RSB has been reported, a composite index for each criterion (i.e., Entry, Establishment, Dispersal, or Magnitude) (C_k) was calculated as the weighted sum of normalized indicators as shown in Eqn (8):

$$C_k = \sum_{i=1}^m w_i \cdot x_{is} \quad (8)$$

Likelihood, composed of three sub-criteria, was calculated using the geometric mean (Eqn (9)) to account for the multiplicative relationships inherent in normalized data:

$$Likelihood = \left(C_{Entry} \times C_{Establishment} \times C_{Dispersal}\right)^{\frac{1}{3}} \quad (9)$$

All three components were treated as sequential constraints on invasion likelihood rather than as fully compensatory dimensions. This formulation was motivated by the conceptual structure of the invasion process.[16,17,45] Consistent with this logic, OECD/JRC[58] noted that geometric aggregation is more appropriate when a certain degree of non-compensability is required for composite indicators.

As an additional check, we compared the original geometrically aggregated Likelihood with a simple weighted average Likelihood. The two versions of Likelihood values were reasonably concordant (Spearman's $\rho = 0.79$).

2.6.4 *The final risk index and data analysis*

The final risk index was then calculated according to Eqn (1). To differentiate national risk levels, country-level risk values (Risk) were classified into five categories using the Jenks natural breaks method: very low (≤0.05), low (0.05–0.14), medium (0.14–0.23), high (0.23–0.35), and very high (>0.35). The proposed categories were considered valid as both mean and median Risk values were 0.25 across historically introduced countries (Australia = 0.20, Spain = 0.35, France = 0.33, Hungary = 0.22, Iran = 0.29, Iraq = 0.19, Papua New Guinea = 0.12, and Portugal = 0.32).

After constructing the final risk index framework, leave-one-out sensitivity analysis was conducted.[59] Each indicator was sequentially removed within its corresponding criterion, and the Risk value was recalculated after re-normalizing weights for each criterion. Then, the relative importance of each indicator was assessed by comparing the recalculated Risk values with the original values using Spearman's ρ and mean absolute error (MAE).

To examine continental-scale patterns, a boxplot analysis was conducted to compare the distributions of the final Risk values, and the three Likelihood sub-criteria across continents. Continental boundaries were defined following Mataveli's scheme[60] (Supplementary 7). Additionally, a ternary plot analysis was performed to assess the proportional composition of Entry, Establishment, and Dispersal. A ternary coordinate system was constructed using the three Likelihood sub-criterion to allow for a proportional comparison of their relative contributions. Lastly, a scatter plot analysis was performed to examine the relationship between Likelihood and Magnitude across countries.

The software packages used for geospatial data processing and visualization are listed in Supplementary 8.

3 RESULTS

3.1 CLIMEX results: Ecoclimatic suitability

CLIMEX effectively captured the current distribution of RSB in its native Asian range (Fig. 4(A)). The projected distribution aligned well with the previously reported northern limit in the Russian Far East, situated at approximately 50° N. EI values were notably high across East Asian monsoon regions including Korea, Japan, eastern to southern China, and the Indochina Peninsula, where sufficient precipitation and warm temperatures provide favorable conditions for establishment. EI were particularly high in the

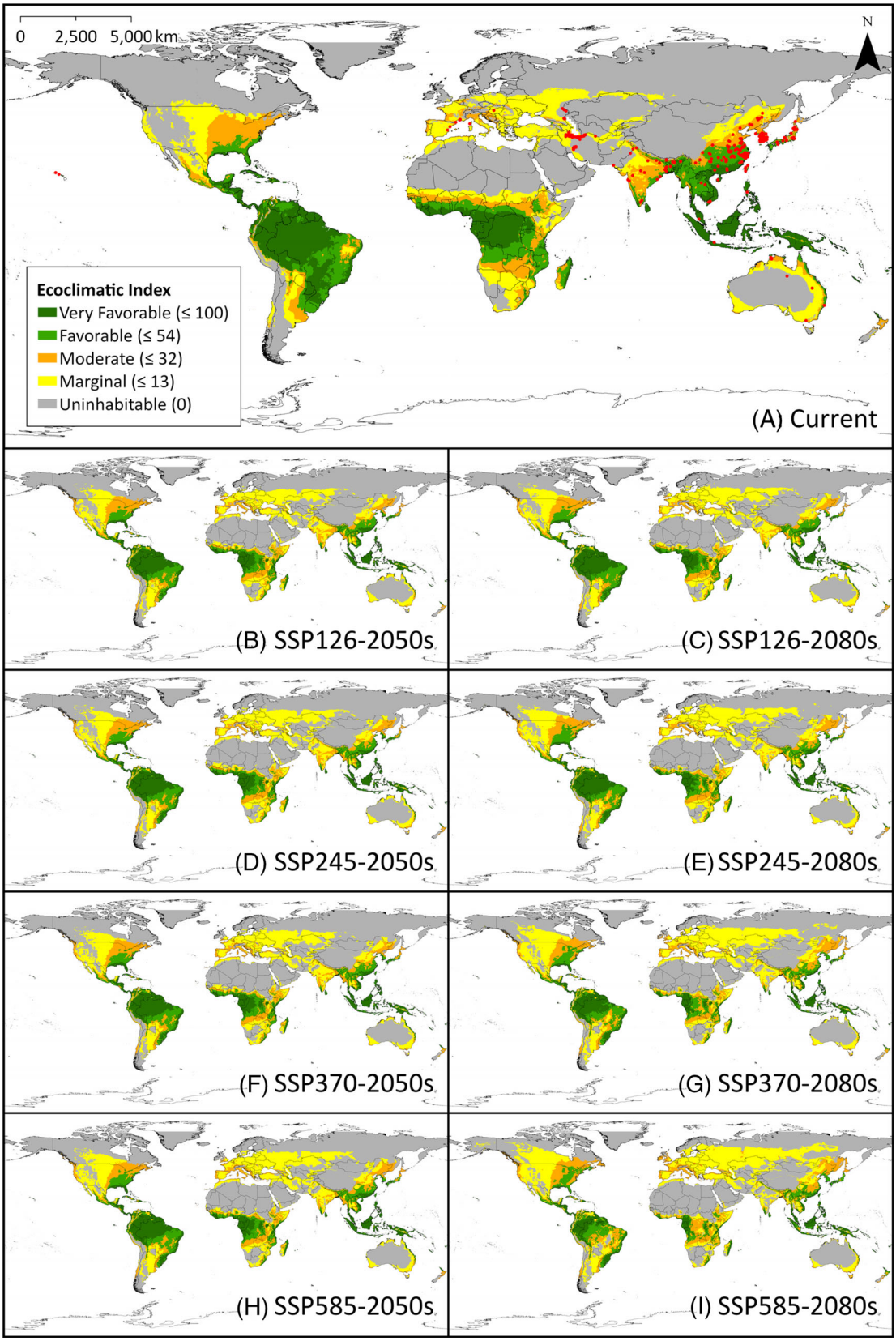

Figure 4. Ecoclimatic suitability of *Chilo suppressalis* under current conditions (A) and future climate scenarios: SSP126 (B–C), SSP245 (D–E), SSP370 (F–G), and SSP585 (H–I). Colors denote suitability classes: grey (uninhabitable), orange (marginal), yellow (moderate), green (favorable), and dark green (very favorable).

Pest Management Science published by John Wiley & Sons Ltd on behalf of Society of Chemical Industry.

Table 3. CLIMEX sensitivity analysis results for *Chilo suppressalis* within study domains

Parameter	Abbreviation	Test range			Sensitivity		
		Low	Default	High	EI[a]	Range[b]	CD[c]
Limiting low temperature	DV0	9	10	11	2.3	2.4	0
Lower optimal temperature	DV1	23	24	25	1.9	0.1	0
Upper optimal temperature	DV2	30	31	32	**3.9**	0.1	0
Limiting high temperature	DV3	35	36	37	1.2	0.2	0
Limiting low moisture	SM0	0.05	0.15	0.25	2.5	**3.4**	0
Lower optimal moisture	SM1	0.7	0.8	0.9	1.7	0.3	0
Upper optimal moisture	SM2	1.9	2	2.1	0.5	0	0
Limiting high moisture	SM3	2.4	2.5	2.6	0.3	0	0
Cold Stress Temperature Threshold	TTCS	−21	−20	−19	0.2	0.1	1
Cold Stress Temperature Rate	THCS	−0.0012	−0.001	−0.0008	0.1	0.1	0.1
Heat Stress Temperature Threshold	TTHS	35	36	37	1.2	0.2	0.1
Heat Stress Temperature Rate	THHS	0.0008	0.001	0.0012	0.3	0.1	0
Dry Stress Threshold	SMDS	0.05	0.15	0.25	2.8	1.3	**9.2**
Dry Stress Rate	HDS	−0.006	−0.005	−0.004	0.6	0.2	0.4
Wet Stress Threshold	SMWS	2.4	2.5	2.6	0.1	0	0
Wet Stress Rate	HWS	0.0016	0.002	0.0024	0.1	0	0
Degree-days per Generation	PDD	672.27	840.34	1008.4	2	2.7	0

Note: Values in bold are the most sensitive parameters in each test.
[a] Percent change of the Ecoclimatic Index (EI): The sensitivity of the overall climatic suitability.
[b] Percent change of the Range: Locations that EI is 1 or more.
[c] Percent change of the Core Distribution (CD): Locations that are warm enough to complete at least one generation, and do not accumulate any stress.

Table 4. Changes in area by Ecoclimatic Index (EI) classes of *Chilo suppressalis* under different shared socioeconomic pathways

Unit: million km^2

Suitability Class (EI)	Current	SSP126		SSP245		SSP370		SSP585	
		2050s	2080s	2050s	2080s	2050s	2080s	2050s	2080s
Total Inhabitable (0 <)	65.5	68.6	69.5	69.6	71.9	69.4	72.8	70.4	73.6
Very Favorable (55–100)	19.1	15.6	15.9	15.6	14.8	15.6	13.0	15.5	9.7
	14.3%	11.7%	11.9%	11.7%	11.1%	11.7%	9.7%	11.6%	7.3%
Favorable (33–54)	13.1	12.2	12.0	12.0	11.9	12.0	12.0	11.9	11.6
	9.8%	9.1%	9.0%	9.0%	8.9%	9.0%	9.0%	8.9%	8.7%
Moderate (14–32)	12.9	15.2	14.4	15.1	16.2	14.7	16.4	14.7	18.1
	9.7%	11.4%	10.8%	11.3%	12.1%	11%	12.3%	11%	13.6%
Marginal (1–13)	20.3	25.6	27.2	26.9	29.0	27.2	31.5	28.4	34.2
	15.2%	19.2%	20.4%	20.2%	21.7%	20.4%	23.6%	21.3%	25.6%
Uninhabitable (0)	68.0	64.9	64.0	63.8	61.6	64.1	60.7	63.0	59.9
	51.0%	48.6%	47.9%	47.8%	46.1%	48%	45.4%	47.2%	44.9%

equatorial Pacific region, reflecting RSB's strong association with moist, thermally suitable environments. In contrast, climatic constraints were evident in Pakistan and Iran, where high temperatures combined with limited precipitation drive significant heat and dry stress. These geographic patterns are consistent with the known ecological requirements of RSB and support the ecological plausibility of the CLIMEX model.

The sensitivity analysis indicated that the model response was primarily driven by the upper limit of temperature optimality and dry stress (Table 3). The most sensitive parameter regarding EI change was the upper optimal temperature (DV2), which resulted in 3.9% change, followed by the dry stress threshold (SMDS) at 2.8% of. Because DV2 controls the upper end of the temperature optimality, this parameter likely accounts for the decrease EI in the tropics under climate change scenarios due to increasing temperature. Furthermore, the lower moisture limit (SM0) had the greatest impact on the Range change (3.4%), while SMDS was the most sensitive parameter for changes in the Core Distribution (9.2%). Since both parameters govern dryness threshold, these results suggest that irrigation in agricultural areas could enhance the RSB survivorship in arid regions of South, Central, and West Asia. Overall, the sensitivity analysis highlights the strong dependence of RSB on humid environments, consistent with its close association with irrigated cropping systems such as rice paddies.

Table 5. Area of individual stress accumulations and percentage of uninhabitable area.

Unit: million km^2

Stress	Current	SSP126		SSP245		SSP370		SSP585	
		2050s	2080s	2050s	2080s	2050s	2080s	2050s	2080s
Cold Stress	28.2*	25.1	23.6	24.0	21.4	23.5	18.9	22.7	16.0
	48.7%†	41.5%	42.4%	41.9%	34.6%	42%	27.3%	38.9%	19.7%
Dry Stress	73.6	72.0	72.3	73.6	73.8	73.5	76.0	74.0	78.5
	26.8%	29.5%	28.9%	28.2%	27.7%	28.7%	27.3%	28.4%	27.6%
Heat Stress	24.5	30.1	31.7	31.4	37.2	32.1	44.0	34.4	53.0
	18.1%	23.6%	25.5%	23.5%	32.5%	24.7%	36.2%	29.6%	40.3%
Wet Stress	0.3	0.7	0.7	0.7	0.8	0.7	0.8	0.8	0.8
	0.1%	7.2%	7.1%	7.3%	8.1%	7.3%	8.6%	7.2%	10.4%

*Area of stress accumulation (stress >0).
† Percentage of uninhabitable area (stress = 100).

With climate change, the global inhabitable area (EI > 0) is projected to expand from 65.5 to 73.6 million km^2 by the 2080s under SSP585 (Table 4). However, the proportions of favorable and very favorable areas declined from 9.8% and 14.3% to 8.7% and 7.3%, respectively, under SSP585 − 2080s. Thus, severe climate change is expected to broaden the potential range of RSB while reducing the proportion of highly suitable regions. Detailed continental results are summarized in Supplementary 9.

Of the four CLIMEX stress factors (see Supplementary 10–13), dry stress (DS) is predicted to dominate both at present (73.6 million km^2) and in the future (78.5 million km^2 under SSP585-2080s) (Table 5). Currently, cold stress (CS) and heat stress (HS) affect less than half the DS area (28.2 and 24.5 million km^2, respectively). Climate change is projected to reverse this trend, reducing CS to 16.0 million km^2 while sharply increasing HS to 53.0 million km^2 by SSP585-2080s. Wet stress (WS) remains negligible, affecting less than 1 million km^2 under all SSPs.

Regional differences in ecoclimatic suitability are evident. In Asia and Oceania, EI is expected to decline in tropical regions such as South Asia and the Indochina Peninsula, while marginal-to-moderate suitability expands northward into southern Russia and Central Asia. In Europe, EI improves, particularly in the south and east, suggesting Central Europe and southern Scandinavia could soon be vulnerable to invasion.

Although RSB has not yet been reported in the Americas and Africa, CLIMEX projects high climatic suitability in many regions even under current conditions (Fig. 4(A)). Presently, inhabitable areas include 18.16 million km^2 (60.7% of land) in Africa, 8.3 million km^2 (36.1%) in North America, and 15.2 million km^2 (85.6%) in South America (Supplementary 9). By comparison, Asia's inhabitable area is 16.02 million km^2 (35.8%), suggesting Africa and South America may exceed Asia in potential establishment. Notably, 70.9% of South America is categorized as favorable or very favorable, with climatic conditions largely matching those of RSB's native Asian–Oceanian range, raising significant invasion concerns.

However, favorable and very favorable areas in the Americas and Africa are projected to decline with climate change, particularly in the southern United States, northeastern Brazil, the Sahel, and parts of sub-Saharan Africa (Fig. 4(B)–(I)). Conversely, reduced CS could enable northward expansion into marginal areas such as southern Canada.

3.2 Invasion risk assessment

The final entropy weights for each indicator and leave-one-out sensitivity analysis results are presented in Supplementary 14. Among Entry indicators, inter-country railway connections ($CROSS_{rail}$) contributed most (0.26), followed by trade volume from RSB-distributed regions ($CARGO_{rsb}$), 0.21. For Establishment, both ports (EI_{port}) and croplands ($EI_{cropland}$) contributed equally (0.36). Dispersal was dominated by total railway length ($LENG_{rail}$), 0.68. Magnitude was governed by rice harvest area ($AREA_{rice}$, 0.52) and the proportion of rice harvested area ($PROP_{rice}$, 0.48).

All indicators showed high Spearman's ρ (>0.95) in the sensitivity analysis (Supplementary 14). Within each criterion, $PORT_{water}$ (0.9893), $AREA_{irrig}$ (0.9650), $LENG_{rail}$ (0.9519), and $AREA_{rice}$ (0.9933) showed the lowest ρ, and $CROSS_{rail}$ (0.0118), $AREA_{irrig}$ (0.0127), $LENG_{rail}$ (0.0252), and $AREA_{rice}$ (0.0109) showed the highest MAE for Entry, Establishment, Dispersal, and Magnitude, respectively. Overall, $LENG_{rail}$ was identified as the most sensitive indicator in this framework.

The invasion risk for each country and continent was calculated using the composite risk index (Eqn (8)). As continental risk values were highly skewed with outliers (Fig. 5), the median was used for comparisons. The global risk score was 0.16. Median scores revealed clear continental patterns: South America ranked highest (0.21), followed by Africa (0.18), North America (0.17), Europe (0.08), Asia (0.10), and Oceania (0) (Supplementary 15). Among 147 non-invaded countries, Medium risk was most common (32%), followed by Very Low (27%), Low (19%), High (16%), and Very High (5%) (Fig. 5(A)). South America showed the widest range of risk values, followed by Africa and North America (Fig. 5(B)). Asia and Oceania had relatively low medians, while Europe showed a low median but with several high-risk outliers.

Each criterion offered further insights. Entry risk peaked in Europe (0.69) and Asia (0.51). Establishment was highest in Oceania (0.75), followed by North America (0.64) and South America (0.54). Dispersal was strongest in Europe (0.52). Magnitude underscored South America (0.75), Africa (0.66), and North America (0.62) as highly vulnerable (Fig. 6(A)). Together, these results show that invasion risk emerges from interactions between trade, environmental suitability, transport infrastructure, and rice dependence.

Pest Management Science published by John Wiley & Sons Ltd on behalf of Society of Chemical Industry.

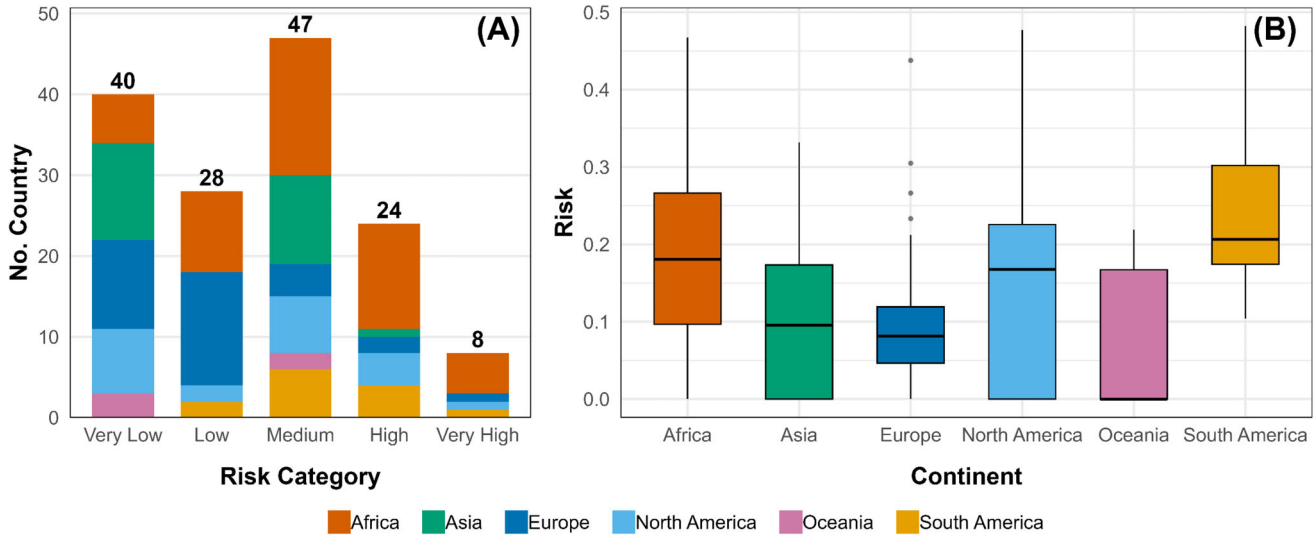

Figure 5. Country-level invasion risk index of *Chilo suppressalis*. The risk metric (Risk) is a unitless index on a 0–1 scale, where higher values indicate greater invasion risk. (A) Stacked bar chart showing the number of countries in each risk category. Risk values are classified into five categories using the natural breaks (Jenks) method: very low (≤0.05), low (0.05–0.14), medium (0.14–0.23), high (0.23–0.35), and very high (>0.35). (B) Boxplots of country-level risk by continent. Colors indicate continents: Africa (vermillion), Asia (bluish green), Europe (blue), North America (sky blue), Oceania (reddish purple), and South America (yellow-orange).

Ternary analysis further revealed continental contrasts (Fig. 6(B)). Asian and European countries clustered along the Entry–Dispersal axis, whereas African and American countries were broadly distributed, reflecting high heterogeneity. These countries also spanned nearly the full range of Likelihood and Magnitude (Fig. 6(C)), underscoring diverse invasion pressures. Collectively, results highlight the Americas and Africa as high-risk regions requiring varied, country-specific management strategies.

3.2.1 *Asia and Oceania: almost overwhelmed*

Overall invasion risks in Asia and Oceania are low. Asia shows high Entry (0.51) and Dispersal (0.44) but the lowest Establishment (0.10) (Supplementary 15), suggesting that most suitable areas are already occupied by RSB. To prevent further spread, rice-growing countries in the Caucasus, Central Asia, and Western Asia (e.g., Afghanistan, Tajikistan, Turkmenistan, Uzbekistan, Azerbaijan, Georgia, Armenia, and Syria) must strengthen measures against RSB dispersal into rice fields (Fig. 7(A)).

In contrast, Oceania shows high Establishment (0.75) but low Entry (0.27). If RSB invade Fiji or the Solomon Islands, substantial economic losses could occur given their high Establishment (Fiji: 0.81; Solomon Islands: 0.76) and Magnitude (Fiji: 0.59; Solomon Islands: 0.51). Quarantine of imports and tourism routes is therefore crucial for prevention.

3.2.2 *Europe: It's not over yet*

Although Europe's overall invasion risk is relatively low, several significant hotspots are projected. Italy (0.44) and Greece (0.30) emerge as high-risk areas due to rice cultivation and well-connected transport networks (Fig. 7(A)). Outside these hotspots, 25 of 32 countries have low or very low Risk values (Fig. 7(A)), largely because of cooler climates and limited rice cultivation.

Europe records the highest Entry (0.69) and Dispersal scores (0.52) (Supplementary 15), indicating strong potential for RSB invasion and rapid spread through transport networks. However, low Establishment (0.19) and Magnitude (0.23) reduce overall risk, suggesting limited population persistence and impacts beyond the identified hotspots.

3.2.3 *Americas and Africa: persistent invasion hotspots*

3.2.3.1. South America. South America shows the highest invasion potential globally (Supplementary 15). Brazil (0.482) ranks as the most at-risk country worldwide due to extensive rice harvest areas, favorable climate, and strong trade connectivity (Fig. 7(A)). Colombia (0.35), Uruguay (0.33), Argentina (0.30), and Bolivia (0.29) also score high. Only Paraguay and French Guiana fall below the global median (<0.16), highlighting the continent's substantial vulnerability.

High invasion risk in South America is strongly linked to Magnitude (0.75) and Establishment (0.54) (Supplementary 15). All countries scored Magnitude >0.5, and 7 of 13 scored Establishment >0.5. In contrast, Entry (0.25) is the second lowest among continents, as natural dispersal of RSB is negligible (PROX = 0).

3.2.3.2. North America. North America exhibits the greatest variation in risk values (Supplementary 15). The United States ranks second globally (0.48), driven by high Entry (0.74), Dispersal (0.82), and Magnitude (0.79). These reflect extensive trade, dense transport infrastructure, and significant rice production. Although Establishment is relatively low (0.36), high cropland suitability ($AREA_{EI9.58} = 0.90$) and irrigated area ($AREA_{irrig} = 0.70$) indicate favorable conditions for persistence. Several Central American countries—including the Dominican Republic, Panama, Costa Rica, and Mexico—also face high risk. In contrast, many Caribbean islands (e.g., Guadeloupe, Martinique, the Bahamas, Saint Lucia, Barbados, Puerto Rico, and Antigua and Barbuda) scored zero due to negligible rice production. Canada's risk is also low (0.04), reflecting limited rice cultivation and harsh climate. This wide risk spectrum, from zero to the global maximum, underscores the continent's heterogeneity.

At the sub-criteria level, North America shows a mixed profile. Overall Entry (0.19) is the lowest globally due to negligible natural dispersal (Supplementary 15). However, the United States

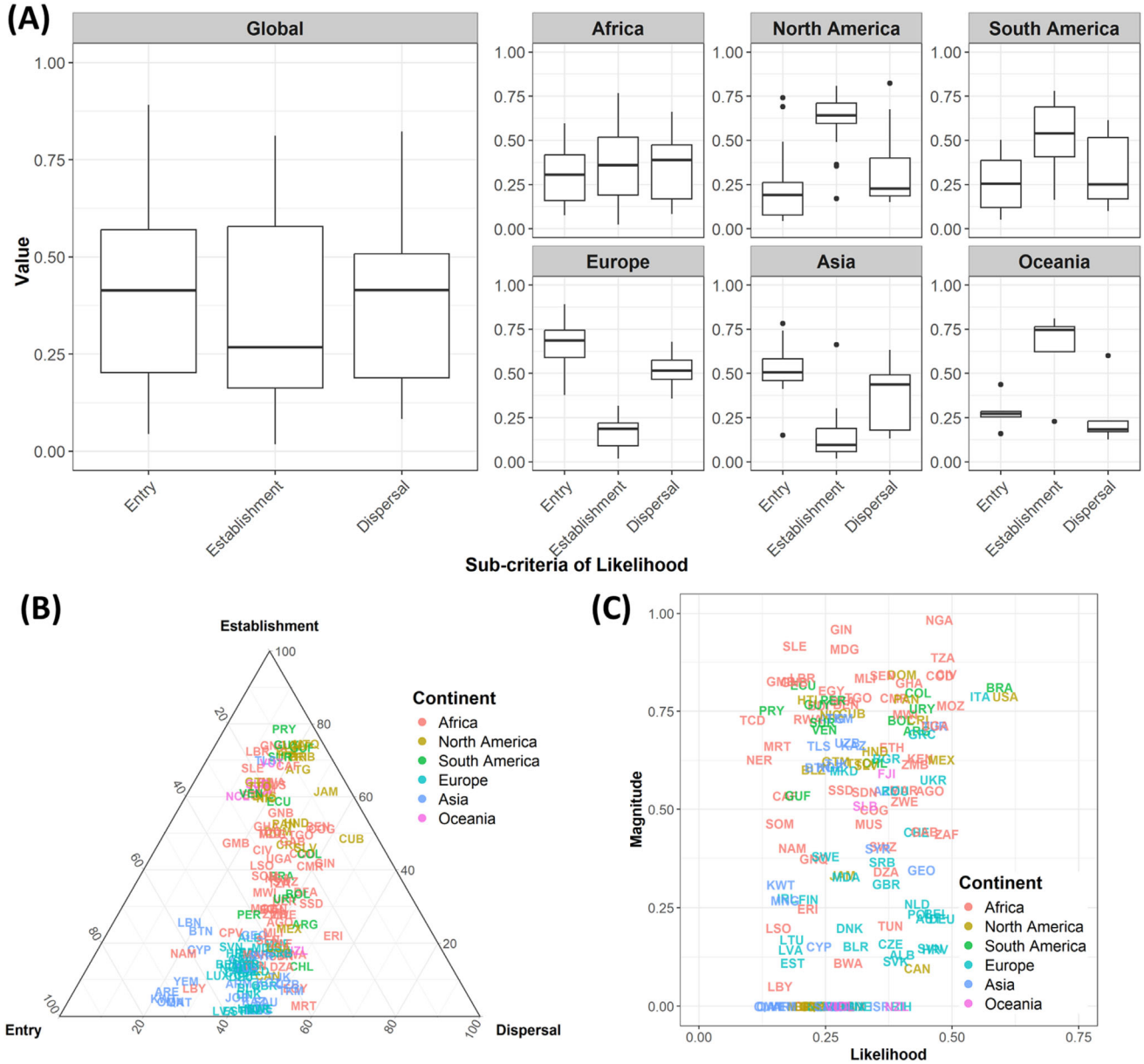

Figure 6. (A) Boxplots of Likelihood factors (Entry, Establishment, Dispersal) across continents. (B) Ternary plot showing proportional contributions of Entry, Establishment, and Dispersal to Likelihood. (C) Scatter plot of Likelihood *versus* Magnitude by country, with ISO3 codes marking positions. Colors in (B) and (C) denote continents. Only countries where *C. suppressalis* invasion has not yet been reported are included.

ranks among the highest globally for import logistics and port activity, which makes human-mediated pathways substantial. When combined with its high Dispersal score (0.82), failure in quarantine could result in secondary spread after establishment. This could cause severe economic damage in countries with high-Magnitude such as the Dominican Republic (0.84), Panama (0.78), and Colombia (0.80).

3.2.3.3. Africa. Africa has the second greatest invasion potential among all continents (Supplementary 15). Major hotspots include Nigeria (0.47), Tanzania (0.43), Côte d'Ivoire (0.41), the Democratic Republic of the Congo (0.40), and Mozambique (0.38) (Fig. 7(A)). In contrast, only 16 of 52 countries have low or very low Risk values. Cape Verde and Comoros scored zero because they do not produce rice. Given that rice is a staple in most sub-Saharan countries, invasion could have serious consequences.

Africa records the highest Magnitude (0.66), reflecting both extensive rice harvest areas and heavy economic dependence on rice (Supplementary 15). Entry, Establishment, and Dispersal (0.31, 0.36, and 0.39, respectively) are close to the global medians (0.41, 0.27, and 0.41), indicating sufficient human-mediated pathways, suitable climates, and spread potential (Supplementary 15). These results position Africa as a critical priority for quarantine and tailored management strategies to prevent and contain emerging invasion fronts.

3.2.4 *Future invasion risk under SSPs*

Future projections under SSPs offer important insights. Globally, median Risk decreases modestly under all SSPs compared to current conditions (Fig. 8). By the 2050s, declines range from −8.4% (SSP126) to −5.8% (SSP585). By the 2080s, declines are greater, ranging from −7.2% (SSP245) to −11.1% (SSP585).

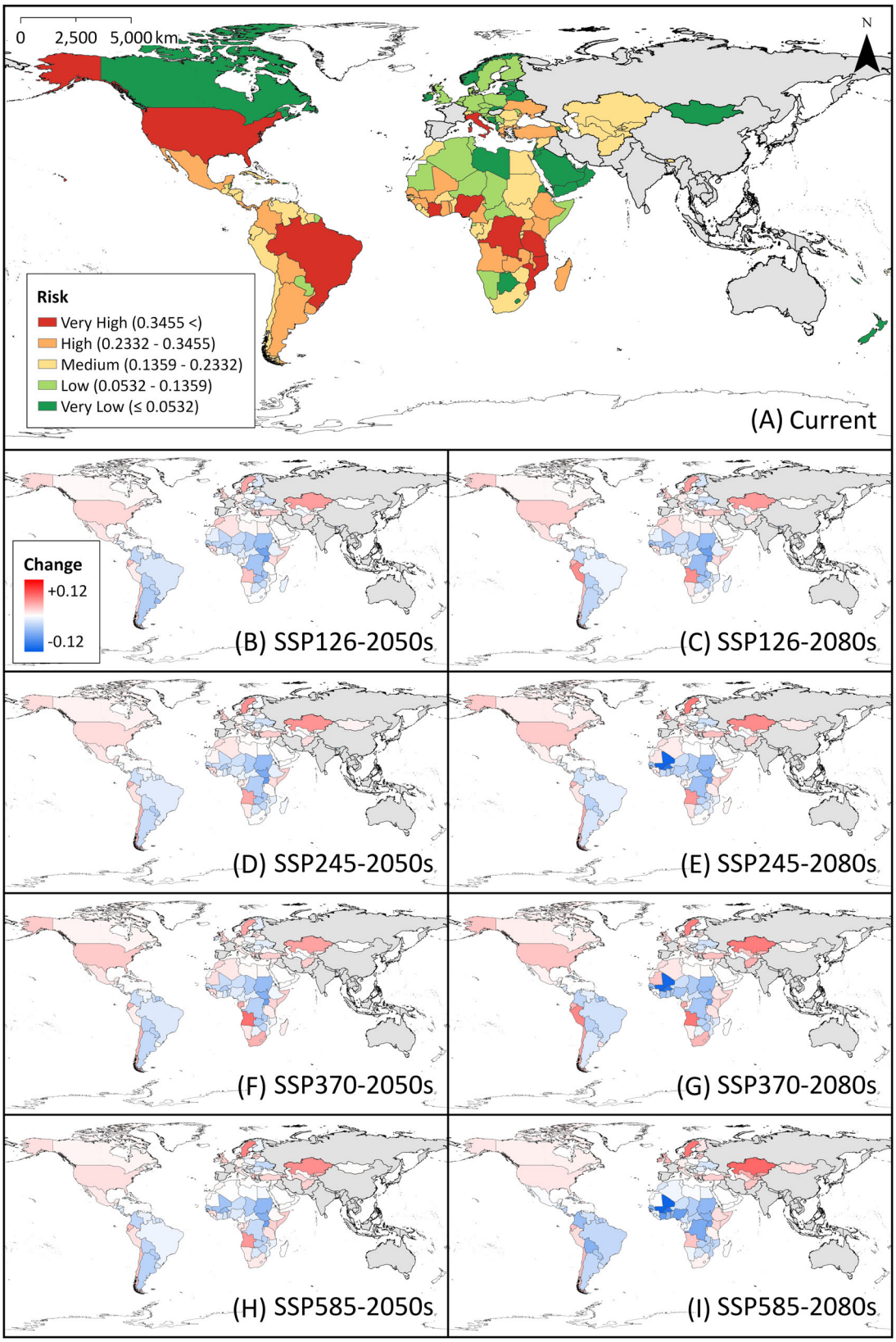

Figure 7. Global invasion risk of *Chilo suppressalis* under current conditions (A) and changes in invasion risk under future climate scenarios: SSP126 (B–C), SSP245 (D–E), SSP370 (F–G), and SSP585 (H–I). In panel A, colors represent risk intensity: green (very low), light green (low), yellow (medium), orange (high), and red (very high). In panels B–I, red shading indicates increasing risk and blue shading indicates decreasing risk.

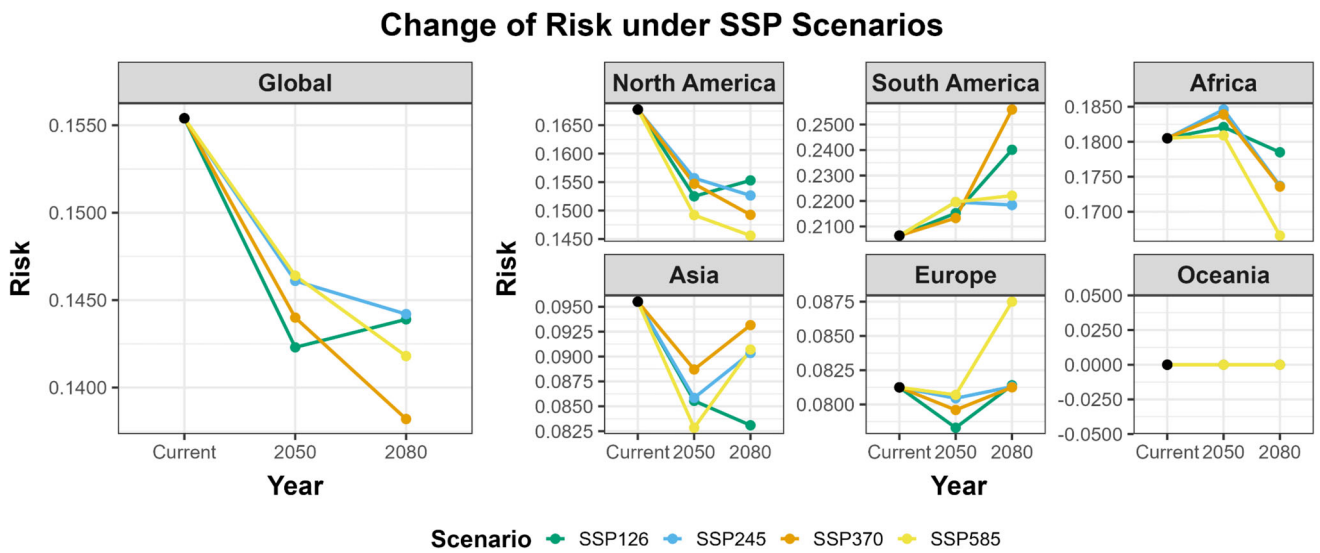

Figure 8. Changes in continental median invasion risk index of *Chilo suppressalis*. The risk metric (Risk) is a unitless index on a 0–1 scale, where higher values indicate greater invasion risk. Green, blue, orange, and yellow represent SSP126, SSP245, SSP370, and SSP585, respectively.

Continental patterns vary (Fig. 8). South America's median Risk rises across all scenarios, increasing from 0.21 to 0.26 under SSP370-2080s (+24%). North America shows the largest decreases, with medians falling by up to −13.2% (SSP585-2080s). Africa's Risk remains stable in the near term but decreases by up to −7.7% (SSP585-2080s). Europe and Asia show dips in the 2050s followed by partial recovery by the 2080s.

At the national level, the sharpest increases occur in high-latitude temperate countries, while equatorial countries show the largest declines (Fig. 7(B)–(I)). Under SSP585-2080s, Kazakhstan (+0.07) and Kyrgyzstan (+0.04) in Asia face significant risk due to proximity to current RSB regions and large rice areas. In Europe, Sweden shows the largest increase (+0.06), though its absolute Risk remains moderate (0.16). Italy consistently remains Europe's highest-risk country (0.45 in SSP585-2080s). In the Americas, changes are modest, with Peru showing the largest increase (+0.06 in SSP370-2080s). Sub-Saharan countries near the equator see the steepest declines due to reduced EIs. Oceania remains stable across all SSPs (Fig. 8).

4 DISCUSSION

This study demonstrated an integrated, multifaceted risk assessment framework for evaluating the global invasion risk of RSB. Our results suggest that RSB has significant potential to become an invasive pest of global concern. Poleward range shifts driven by climate change will likely expand the potential geographic range of RSB; however, a considerable decline in climatic suitability in low latitudes is also expected. The integrated risk assessment indicates that influential factors of invasion risk vary by region, emphasizing the importance of region-specific management. The results also highlight the need to consider both climate and land cover changes. These findings contribute to a broader understanding of climate-driven invasion dynamics and lay the groundwork for targeted biosecurity strategies.

4.1 Key insights from the risk assessment framework

Many studies use SDMs to approximate 'invasion risk' with maps of potential distribution or environmental suitability.[10,61] While useful for identifying potential range limits, this approach overlooks the dynamic, sequential nature of invasions and their impact on exposed assets. Crucial factors such as anthropogenic and socioeconomic elements are often ignored,[62] leading to a static and incomplete view of invasion risk.

Worner and Gevrey[63] employed self-organizing maps (SOMs) to identify regions at risk of new pest invasions based on species co-occurrence assemblage patterns. Their work emphasized ecological similarity between regions as an indicator of susceptibility, suggesting that areas with similar pest compositions might be vulnerable to additional species. While informative, this approach abstracts invasion processes, focusing on spatial patterns rather than actual dynamics. Consequently, it is limited in forecasting future invasions or accounting for shifts in climate, land use, or trade connectivity.

To address these limitations, our study introduced a composite risk index based on the FAO's robust conceptual framework. This is the first study to operationalize the FAO pest-risk concept as a spatially explicit, national-scale composite index. Existing studies often provide only criterion-level descriptions, lacking reproducible, data-driven results that can be compared across countries or updated with new data.[64] Our framework overcomes these limitations by applying explicit normalization and entropy-based weighting, which reduce arbitrariness and reflect indicator variability. This design allows countries to understand their risk scores and supports SSP scenario-based projections under future climate and land-cover change.

The framework also offers methodological and operational advantages. It identifies weak indicators for each country, providing direct input for management strategies. For example, a country with high Entry from the $CARGO_{rsb}$ indicator could adjust straw imports from RSB-free countries. The indicator set is also flexible, allowing substitution or augmentation (e.g., commodity-specific trade flows, new entry pathways) while retaining the core logic.

In short, this framework provides a robust, policy-relevant tool for invasion risk assessment, integrating climate, trade volume, transportation networks, entry pathways, and potential impacts into a single, interpretable index.

Pest Management Science published by John Wiley & Sons Ltd on behalf of Society of Chemical Industry.

4.2 Continental-based RSB invasion risk assessment

4.2.1 Europe

Based on the documented invasion history, occurrence records, and the CLIMEX results, we infer the presence of two main corridors in Europe.[25–28] The first corridor is an invasion from the east, via Iran and Russia.[27,28] Geographical continuity suggests that both natural dispersal and human-mediated introduction could facilitate RSB movement into mainland Europe. Therefore, further investigation is crucial in regions linking the Caucasus to Eastern Europe, which offer suitable conditions for RSB establishment and require targeted monitoring.

The second corridor is an invasion from the west, along the Mediterranean coast from Spain to France.[25,26] This invasion has been ongoing since RSB was first reported in Valencia in the 1930s. However, it remains largely confined to coastal areas, mainly due to limited rice cultivation.[38,65] Together with the limited host availability, cooler thermal conditions in Mediterranean Europe result in lower effective degree-day accumulation than in parts of Western Asia (e.g., northern Iran), where EI values are similar, but RSB occurrences are reported more frequently (Supplementary 16). Although overall precipitation in Europe is higher than in parts of Western Asia, it remains lower than that characteristic of RSB's native range in Asia.[66] Additionally, natural predators, such as insectivorous bats, may also have slowed the expansion.[67] Furthermore, the western Alps may act as a major geographic barrier that limits eastward spread of RSB, which is particularly important given that Italy is the largest rice-producing country (> 227.4 thousand ha) in Europe.[38]

4.2.2 Africa

RSB has not yet been detected in Northern Africa, most likely due to the geographical barriers of the Sinai Peninsula and the Arabian Desert. Furthermore, the region's extremely low annual precipitation and high aridity prevailing across Northern Africa result in very low climatic suitability for establishment, as evidenced by consistently marginal EI values.

However, climatic suitability alone does not fully capture invasion risk in highly managed agricultural systems. In this context, Egypt faces the greatest risk despite its low EI values throughout the country. Egyptian agriculture is highly concentrated along the Nile Delta, where it depends heavily on intensive irrigation and periodic flooding. These practices create localized humid environments that are not captured by CLIMEX modeling. Furthermore, the Nile Delta is one of the world's most productive rice-growing regions, producing over eight tons/ha.[65] These factors indicate that Egypt exhibits high agricultural vulnerability and potential impact following introduction, regardless of general climatic trends. This underscores the necessity of integrating non-climatic risk components into invasion risk assessment. Finally, the cultivation of alternative host crops, such as wheat and maize, could further facilitate RSB establishment. As several rice-feeding Chilo species, including *C. agamemnon* and *C. luteellus*, already cause significant damage in the region,[68] potential competition between RSB and these existing pest species could further shift pest dynamics and increase overall pressure on rice.

Many Sub-Saharan countries depend heavily on rice cultivation and could face severe economic losses. In Madagascar, for example, nearly 85% of farmers are employed in rice farming, which supports over 60% of the population.[69] Tanzania relies on rice as a staple crop, making it particularly vulnerable. Nigeria, with the largest rice-growing area in Africa but low productivity,[65] is also at risk.

4.2.3 Americas

The Americas have remained largely free of RSB, except for severe outbreaks in Hawaii during the 1920s.[24] To date, there is no evidence of establishment on the mainland. However, risk persists, as RSB mandibles have been found in reed screens imported from Japan.[70] This highlights the need for continuous monitoring and strict quarantine measures, especially for straw-based imports.

The economic consequences could be substantial in major rice producers such as Brazil, the United States, Peru, and Argentina.[65] Brazil produces over 10 million tons annually, while the United States ranks among the top 10 global producers, with cultivation concentrated in Arkansas, Louisiana, Mississippi, and Texas. Peru and Argentina also have sizable rice industries.[65] These countries also cultivate maize and wheat, which could further facilitate RSB establishment and spread.[22,38]

4.3 Limitations and future directions

The most significant limitation of our framework is temporal inconsistency among input datasets. The first source of inconsistency arises from the reliance on static socioeconomic and infrastructure inputs for future projections. We assumed that global trade, the ratio of rice harvest areas to croplands, and transport networks would remain constant. However, these factors are expected to change considerably under different SSPs. For instance, SSP1, which promotes an eco-friendly economy and global cooperation, could increase imports in developing countries, thereby raising the risk of RSB introduction.[71] Conversely, SSP3, characterized by regional conflicts and protectionist trade policies, could reduce imports and lower the likelihood of RSB introduction *via* trade routes. Additionally, road expansion is projected to vary significantly across SSPs, from a 14% increase under SSP4 to a 23% increase under SSP5 by 2050.[34] Furthermore, RSB host crop productivity is projected to decline in tropical and subtropical regions due to heat stress and water scarcity, while increasing in high-latitude regions.[72] Together, these inconsistencies indicate that the future risk maps of this study should be interpreted as conditional scenario-based projections rather than precise forecasts. The second inconsistency arises from the intrinsic characteristics of climate data used in SDM studies. While most socioeconomic and infrastructure-related variables in this study reflect conditions after 2000, commonly used global climate datasets for SDMs are based on long-term climatology largely derived from observations before 2000.[42,73,74] For CLIMEX, this issue is further compounded by a shortage of compatible climate datasets, because the model requires relative humidity at two specific times of the day (9:00 and 15:00 h). These limitations highlight the urgent need for temporally synchronized climate-socioeconomic datasets for a more policy-relevant understanding of invasion risk evolution.

Another limitation of this study lies in methodological aspects. First is the absence of an explicit natural dispersal component. For highly mobile or long-range migratory species, Entry and Dispersal could be augmented with air current-related indicators. For example, distance-based decay kernel functions calibrated to flight ability or seasonal wind-trajectory data could help differentiate between human-mediated and natural dispersal. This would also enable the framework to capture episodic, climate-dependent dispersal events not represented by static indicators. Second, the risk index is presented at the national level; consequently, sub-national variation within large countries may be obscured by spatial aggregation.[10] Brazil, for example, is classified as 'very high risk' in our analysis but exhibits pronounced internal

contrasts across key determinants of invasion risk, including transportation, rice-growing areas, and import flows. This spatial heterogeneity suggests that invasion risk is unlikely to be uniform across the country. This limitation is primarily attributable to data availability. To the best of our knowledge, no openly accessible global database currently provides sub-national trade and distribution data or a well-documented sub-national invasion history for RSB. As a result, the invasion risk assessment framework in this study was constructed on a national scale, which provided the most consistent spatial unit for integrating multiple indicators across countries. The national scale is also relevant in practical terms, because invasive pest management is typically implemented through national phytosanitary and policy frameworks.[75] Therefore, the final risk index should be interpreted as a broad indicator of overall invasion pressure at the national scale, rather than a reflection of localized risk level. This limitation could be addressed in future by developing indicators that take geographic heterogeneity into account.

Finally, independent validation of the framework remains challenging. When we explored hindcasting against country-level first-detection years, introduction and establishment data are often uncertain or undocumented. Although most historically introduced countries were categorized as 'high' or 'very high risk' in our validation test (see Section 2.6.4), the temporal coverage of the datasets used in this study did not fully encompass all historical invasion. Future work should focus on curating verifiable event histories to enable formal temporal validation. Encouragingly, advances in quarantine and information technologies—such as electronic phytosanitary certificates, shipment-level trade data, and genomic surveillance—are expected to provide sufficient information for validation.

Despite these limitations, our study presents a practical and policy-relevant framework that supports national-level pest risk management. Because the proposed methodology has flexible structure, we expect this framework could be applied to assess potential invasion risk of other species. For example, the commodity related indicators employed in this case study (e.g., $CARGO_{total}$) are expected to be applicable to other stemboring pests, such as Chilo and Sesamia species,[76] since they have similar entry pathways. In addition, the framework can be further improved into a more standardized methodology by incorporating a broader range of species-specific and pathway-specific indicators. For example, future applications could integrate additional entry-related pathways (e.g., passenger travel for each transportation, live plant trade, and agricultural machinery and goods). Furthermore, when this framework is established for multiple species, the resulting database is expected to inform trade partner portfolio strategies aimed at minimizing quarantine burden and reducing the risk of potential economic damage. By enabling consistent and transparent integration of risk components, this framework provides a useful foundation for proactive invasion risk assessment.

5 CONCLUSION

We developed a national-level, composite invasion risk assessment framework based on the FAO invasion risk concept and applied it to assess the global invasion risk of *Chilo suppressalis* (RSB). The results indicate that RSB poses a significant invasion threat to South America, Africa, and North America. Furthermore, our findings suggest that future invasion risk will vary across SSP scenarios.

Our results provide two key insights. First, RSB has the potential to become a globally invasive pest. Second, invasion risk is determined by multiple interacting factors rather than a single driver. This explains why some regions far from a pest's native range are highly vulnerable due to strong establishment potential or significant expected impact, while certain nearby areas show relatively low risk. These findings underscore the necessity of developing country-specific biosecurity strategies.

Despite offering valuable insights, the current framework has some limitations. It relies largely on static trade and transportation data and lacks indicators for natural dispersal. Additionally, validation is constrained by the scarcity of detailed historical invasion records and raw data for hindcasting. Future work should incorporate specific trajectories for trade, transport networks, and rice production under different SSP scenarios. We also recommend integrating dispersal kernels and wind-trajectory indicators to improve accuracy.

Overall, our invasion risk index framework provides policy-relevant information for prioritizing surveillance and targeting interventions. The framework can be generalized to other invasive species and refined as more socioeconomic and ecological data become available.

ACKNOWLEDGEMENTS

The authors acknowledge the World Climate Research Programme's Working Group on Regional Climate and the Working Group on Coupled Modelling, which organized CMIP6. We thank the climate modelling groups for producing and sharing their outputs. We also acknowledge the Earth System Grid Federation (ESGF) infrastructure, an international effort led by the U.S. Department of Energy's Program for Climate Model Diagnosis and Intercomparison, the European Network for Earth System Modelling, and other partners in the Global Organization for Earth System Science Portals (GO-ESSP). This work was supported by the Korea Environment Industry & Technology Institute (KEITI) through the Climate Change R&D Project for the New Climate Regime, funded by the Korea Ministry of Climate, Energy and Environment (MCEE) (RS-2022-KE002294). This research was also supported by the Core Research Institute Basic Science Research Program through the National Research Foundation of Korea, funded by the Ministry of Education (RS-2021-NR060142).

DATA AVAILABILITY STATEMENT

The data that support the findings of this study are available from the corresponding author upon reasonable request.

CONFLICT OF INTEREST

The authors declare no conflict of interest.

SUPPORTING INFORMATION

Supporting information may be found in the online version of this article.

REFERENCES

1 Hulme PE, Trade, transport and trouble: managing invasive species pathways in an era of globalization. *J Appl Ecol* **46**:10–18 (2009). https://doi.org/10.1111/j.1365-2664.2008.01600.x.
2 Paini DR, Sheppard AW, Cook DC, De Barro PJ, Worner SP and Thomas MB, Global threat to agriculture from invasive species. *Proc*

Pest Management Science published by John Wiley & Sons Ltd on behalf of Society of Chemical Industry.

Natl Acad Sci U S A **113**:7575–7579 (2016). https://doi.org/10.1073/pnas.1602205113.
3 Simberloff D, Why are biological invasions important? in *Invasive Species: What Everyone Needs to Know*. Oxford University Press, Oxford, United Kingdom, pp. 9–19 (2013).
4 WTO, *Evolution of World Trade*. World Trade Organization, Geneva, Switzerland. https://www.wto.org/english/res_e/statis_e/trade_evolution_e/evolution_trade_wto_e.htm, (2025).
5 Zenni RD, Essl F, García-Berthou E and McDermott SM, The economic costs of biological invasions around the world. *NeoBiota* **67**:1–9 (2021). https://doi.org/10.3897/neobiota.67.69971.
6 Bradshaw CJA, Leroy B, Bellard C, Roiz D, Albert C, Fournier A *et al.*, Massive yet grossly underestimated global costs of invasive insects. *Nat Commun* **7**:12986 (2016). https://doi.org/10.1038/ncomms12986.
7 Baxter PW and Possingham HP, Optimizing search strategies for invasive pests: learn before you leap. *J Appl Ecol* **48**:86–95 (2011). https://doi.org/10.1111/j.1365-2664.2010.01893.x.
8 Hellmann JJ, Byers JE, Bierwagen BG and Dukes JS, Five potential consequences of climate change for invasive species. *Conserv Biol* **22**: 534–543 (2008). https://doi.org/10.1111/j.1523-1739.2008.00951.x.
9 Skendžić S, Zovko M, Živković IP, Lešić V and Lemić D, The impact of climate change on agricultural insect pests. *Insects* **12**:440 (2021). https://doi.org/10.3390/insects12050440.
10 Venette RC, Kriticos DJ, Magarey RD, Koch FH, Baker RHA, Worner S *et al.*, Pest risk maps for invasive alien species: a roadmap for improvement. *Bioscience* **60**:349–362 (2010). https://doi.org/10.1525/bio.2010.60.5.5.
11 Elith J and Leathwick JR, Species distribution models: ecological explanation and prediction across space and time. *Annu Rev Ecol Evol Syst* **40**: 677–697 (2009). https://doi.org/10.1146/annurev.ecolsys.110308.120159.
12 Guisan A, Thuiller W and Zimmermann NE, Overview of the habitat suitability modeling procedure, in *Habitat Suitability and Distribution Models: With Applications in R*. Cambridge University Press, Cambridge, United Kingdom, pp. 11–20 (2017).
13 Srivastava V, Lafond V and Griess VC, Species distribution models (SDM): applications, benefits and challenges in invasive species management, in *Invasive Species Reviews 2018–2024*, ed. by Hemming D. CAB International, Wallingford, United Kingdom, pp. 239–255 (2019). https://doi.org/10.1079/PAVSNNR201914020.
14 Jiménez-Valverde A, Peterson AT, Soberón J, Overton JM, Aragón P and Lobo JM, Use of niche models in invasive species risk assessments. *Biol Invasions* **13**:2785–2797 (2011). https://doi.org/10.1007/s10530-011-9963-4.
15 Early R, Bradley BA, Dukes JS, Lawler JJ, Olden JD, Blumenthal DM *et al.*, Global threats from invasive alien species in the twenty-first century and national response capacities. *Nat Commun* **7**:12485 (2016). https://doi.org/10.1038/ncomms12485.
16 FAO, *International Standards for Phytosanitary Measures: Framework for Pest Risk Analysis (ISPM No. 2)*. Food and Agriculture Organization of the United Nations, Rome, Italy (2019a).
17 Blackburn TM, Pyšek P, Bacher S, Carlton JT, Duncan RP, Jarošík V *et al.*, A proposed unified framework for biological invasions. *Trends Ecol Evol* **26**:333–339 (2011). https://doi.org/10.1016/j.tree.2011.03.023.
18 Dale D, Insect pests of the rice plant - their biology and ecology, in *Biology and Management of Rice Insects*, ed. by Heinrichs EA. Wiley Eastern Ltd and IRRI, India and Manila, Philippines, pp. 363–485 (1994).
19 Pathak MD, Ecology of common insect pests of rice. *Annu Rev Entomol* **13**:257–294 (1968).
20 Zhu KX, Jiang S, Han L, Wang MM and Wang XY, Fine-scale genetic structure of the overwintering Chilo suppressalis in the typical bivoltine areas of northern China. *PLoS One* **15**:e0243999 (2020a). https://doi.org/10.1371/journal.pone.0243999.
21 Khan ZR, *World Bibliography of Rice Stem Borers: 1794-1990*. International Rice Research Institute and International Centre of Insect Physiology and Ecology, Manila, Philippines (1991).
22 CABI, *Chilo suppressalis*, in *Invasive Species Compendium*. CAB International, Wallingford, United Kingdom (2007). https://doi.org/10.1079/cabicompendium.12855.
23 Van Zwaluwenburg RH, Rust EW and Rosa JS, Notes on the rice-borer, *Chilo simplex*. *Hawaiian For Agric* **25**:79–82 (1928).
24 Yasumatsu K, Nishida T and Bess HA, On the extinction of the Asiatic rice borer *Chilo suppressalis* in Hawaii. *Proc Hawaii Entomol Soc* **20**: 239–245 (1968).
25 Gómez C, El barrenador del arroz. *Bol Patol Veg Entomol Agric* **9**:51–66 (1940).
26 Casagrande E, The commercial implementation of mating disruption for the control of the rice stem borer, *Chilo suppressalis*, in rice in Spain. *Bull OILB SROP* **16**:82–89 (1993).
27 Ebert G, The rice stem borer *Chilo suppressalis* Walker (Lep./Pyral.), a new pest for Iran. *Entomol Phytopathol Appl* **35**:1–25 (1973).
28 Izhevsky SS and Maslyakov VY, New invasions of alien insects into the European part of Russia. *Russ J Biol Invasions* **1**:68–73 (2010). https://doi.org/10.1134/S2075111710020037.
29 Kriticos DJ, Maywald GF, Yonow T, Zurcher EJ, Herrmann NI and Sutherst RW, *CLIMEX Version 4: Exploring the Effects of Climate on Plants, Animals and Diseases*. CSIRO, Canberra, Australia, p. 184 (2015).
30 Sutherst RW and Maywald GF, A computerised system for matching climates in ecology. *Agric Ecosyst Environ* **13**:281–299 (1985). https://doi.org/10.1016/0167-8809(85)90016-7.
31 WITS, World Integrated Trade Solution https://wits.worldbank.org [accessed 5 February 2025].
32 NGA, World Port Index, *Maritime Safety Information. National Geospatial-Intelligence Agency*, Springfield, Virginia (2019) https://msi.nga.mil/Publications/WPI [accessed 9 January 2025].
33 WBG, *Global Airports: Locations of Airports with International Travel. Version 2*. World Bank Group, Washington, DC (2020). https://datacatalog.worldbank.org/search/dataset/0038117 [accessed 5 February 2025].
34 Meijer JR, Huijbregts MA, Schotten KC and Schipper AM, Global patterns of current and future road infrastructure. *Environ Res Lett* **13**: 064006 (2018). https://doi.org/10.1088/1748-9326/aabd42.
35 ArcGIS Hub, World railroads https://www.arcgis.com/home/item.html?id=5ef3425348954c84a45860bcf86c78ab [accessed 21 January 2025].
36 Chen G, Li X and Liu X, Global land projection based on plant functional types with a 1-km resolution under socio-climatic scenarios. *Sci Data* **9**:125 (2022). https://doi.org/10.1038/s41597-022-01208-6.
37 Siebert S, Henrich V, Frenken K and Burke J, *Global Map of Irrigation Areas version 5*. Rheinische Friedrich-Wilhelms-University, Bonn, Germany / Food and Agriculture Organization of the United Nations,Rome, Italy (2013).
38 Tang FH, Nguyen TH, Conchedda G, Casse L, Tubiello FN and Maggi F, CROPGRIDS: a global geo-referenced dataset of 173 crops. *Sci Data* **11**:413 (2024). https://doi.org/10.1038/s41597-024-03247-7.
39 GBIF, GBIF occurrence download (2024). https://doi.org/10.15468/dl.72qzza.
40 O'Neill BC, Kriegler E, Ebi KL, Kemp-Benedict E, Riahi K, Rothman DS *et al.*, The roads ahead: narratives for shared socioeconomic pathways describing world futures in the 21st century. *Glob Environ Change* **42**:169–180 (2017). https://doi.org/10.1016/j.gloenvcha.2015.01.004.
41 Riahi K, van Vuuren DP, Kriegler E, Edmonds J, O'Neill BC, Fujimori S *et al.*, The shared socioeconomic pathways and their energy, land use, and greenhouse gas emissions implications: an overview. *Glob Environ Change* **42**:153–168 (2017). https://doi.org/10.1016/j.gloenvcha.2016.05.009.
42 Kriticos DJ, Webber BL, Leriche A, Ota N, Macadam I, Bathols J *et al.*, CliMond: global high-resolution historical and future scenario climate surfaces for bioclimatic modelling. *Methods Ecol Evol* **3**:53–64 (2012). https://doi.org/10.1111/j.2041-210X.2011.00134.x.
43 Cinquini L, Crichton D, Mattmann C, Harney J, Shipman G, Wang F *et al.*, The earth system grid federation: an open infrastructure for access to distributed geospatial data. *Future Gener Comput Syst* **36**:400–417 (2014). https://doi.org/10.1016/j.future.2013.07.002.
44 Voldoire A, *CNRM-CERFACS CNRM-CM6-1-HR model output prepared for CMIP6 HighResMIP. Version 20240916*. Earth System Grid Federation, Livermore, California (2019). https://doi.org/10.22033/ESGF/CMIP6.1387.
45 FAO, *International Standards for Phytosanitary Measures: Pest Risk Analysis for Quarantine Pests (ISPM No. 11)*. Food and Agriculture Organization, Rome, Italy (2019b).
46 Kanno H and Sato A, Mating behaviour of the rice stem borer moth, *Chilo suppressalis* WALKER (Lepidoptera: Pyralidae) II. Effects of temperature and relative humidity on mating activity. *Appl Entomol Zool* **14**:419–427 (1979). https://doi.org/10.1303/aez.14.419.
47 Ye YL and Wang HX, Regressive parabola model of effects of temperature and humidity on survival rate and fecundity in *Chilo suppressalis* (Walker). *Acta Agric Jiangxi* **19**:31–32 (2007).

48 Atapour M and Moharramipour S, Changes of cold hardiness, supercooling capacity, and major cryoprotectants in overwintering larvae of *Chilo suppressalis* (Lepidoptera: Pyralidae). *Environ Entomol* **38**: 260–265 (2009). https://doi.org/10.1603/022.038.0132.

49 Hong J, Lee M, Kim Y, Lee YS, Wee J, Park JJ *et al*., Potential range shift of a long-distance migratory rice pest, *Nilaparvata lugens*, under climate change. *Sci Rep* **14**:11531 (2024). https://doi.org/10.1038/s41598-024-62266-x.

50 Shamakhi L, Zibaee A, Karimi-Malati A and Hoda H, A laboratory study on the modeling of temperature-dependent development and antioxidant system of *Chilo suppressalis* (Lepidoptera: Crambidae). *J Insect Sci* **18**:35 (2018). https://doi.org/10.1093/jisesa/iey027.

51 Yonow T, Kriticos DJ, Ota N, Van Den Berg J and Hutchison WD, The potential global distribution of *Chilo partellus*, including consideration of irrigation and cropping patterns. *J Pest Sci* **90**:459–477 (2017). https://doi.org/10.1007/s10340-016-0801-4.

52 Zou Y, Ge X, Guo S, Zhou Y, Wang T and Zong S, Impacts of climate change and host plant availability on the global distribution of *Brontispa longissima* (Coleoptera: Chrysomelidae). *Pest Manag Sci* **76**: 244–256 (2020). https://doi.org/10.1002/ps.5503.

53 Jenks GF, The data model concept in statistical mapping. *Int Yearb Cartogr* **7**:186–190 (1967).

54 Wang Y, Li Z, Tang Z and Zeng G, A GIS-based spatial multi-criteria approach for flood risk assessment in the Dongting Lake region, Hunan, Central China. *Water Resour Manage* **25**:3465–3484 (2011). https://doi.org/10.1007/s11269-011-9866-2.

55 Zhang Z, Hu B and Qiu H, Comprehensive assessment of ecological risk in southwest Guangxi-Beibu bay based on DPSIR model and OWA-GIS. *Ecol Indic* **132**:108334 (2021). https://doi.org/10.1016/j.ecolind.2021.108334.

56 Zhu Y, Tian D and Yan F, Effectiveness of entropy weight method in decision-making. *Math Probl Eng* **2020**:3564835 (2020b). https://doi.org/10.1155/2020/3564835.

57 Joanes DN and Gill CA, Comparing measures of sample skewness and kurtosis. *J R Stat Soc: Ser D* **47**:183–189 (1998). https://doi.org/10.1111/1467-9884.00122.

58 OECD/JRC, *Handbook on Constructing Composite Indicators: Methodology and User Guide*. OECD Publishing, Paris (2008). https://doi.org/10.1787/9789264043466-en.

59 Lu M, How new quality productivity drives China's sustainable development: evidence from dynamic indicator evolution. *PLoS One* **20**: e0338804 (2025). https://doi.org/10.1371/journal.pone.0338804.

60 Mataveli G, Worldwide Geographic Division: Continents and Oceans/Seas Shapefile [data set]. Zenodo (2024). https://doi.org/10.5281/zenodo.10778079.

61 Kriticos D, Szyniszewska A, Bradshaw C, Li C, Verykouki E, Yonow T *et al*., Modelling tools for including climate change in pest risk assessments. *EPPO Bull* **54**:38–51 (2024). https://doi.org/10.1111/epp.12994.

62 Hui C, The dos and don'ts for predicting invasion dynamics with species distribution models. *Biol Invasions* **25**:947–953 (2023). https://doi.org/10.1007/s10530-022-02976-3.

63 Worner SP and Gevrey M, Modelling global insect pest species assemblages to determine risk of invasion. *J Appl Ecol* **43**:858–867 (2006). https://doi.org/10.1111/j.1365-2664.2006.01202.x.

64 Poggi S, Desneux N, Jactel H, Tayeh C and Verheggen F, A nationwide pest risk analysis in the context of the ongoing Japanese beetle invasion in continental Europe: the case of metropolitan France. *Front Insect Sci* **2**:1079756 (2022). https://doi.org/10.3389/finsc.2022.1079756.

65 Laborte AG, Gutierrez MA, Balanza JG, Saito K, Zwart SJ, Boschetti M *et al*., RiceAtlas, a spatial database of global rice calendars and production. *Sci Data* **4**:170074 (2017). https://doi.org/10.1038/sdata.2017.74.

66 Dobler A andAhrens B, Precipitation by a regional climate model and bias correction in Europe and South Asia *Meteorol Z* **17**:499–509 (2008). https://doi.org/10.1127/0941-2948/2008/0306

67 Tuneu-Corral C, Puig-Montserrat X, Flaquer C, Mata VA, Rebelo H, Cabeza M *et al*., Bats and rice: quantifying the role of insectivorous bats as agricultural pest suppressors in rice fields. *Ecosyst Serv* **66**:101603 (2024). https://doi.org/10.1016/j.ecoser.2024.101603.

68 Metwally MM, Ecological studies on lepidopterous stem borers associated with the main graminaceous weeds and crops at Kafr El-Sheikh region. *J Plant Prot Pathol* **1**:319–330 (2010).

69 Minten B, Dabat MH and Razafintsalama Z, The rice economy of Madagascar, in *Rice Markets in Madagascar: Policy Options for Increased Efficiency and Price Stabilization*, Africa Region Working Paper Series No. **101**, ed. by Minten B and Dorosh P. World Bank, Washington, DC, pp. 2–10 (2006).

70 PERC, The Purdue Entomological Research Collection, Occurrence dataset 10.15468/hyexfq [accessed via GBIF.org on 20 August 2025] https://www.gbif.org/occurrence/3128640859.

71 Kramel D, Franz SM, Klenner J, Muri H, Münster M and Strømman AH, Advancing SSP-aligned scenarios of shipping toward 2050. *Sci Rep* **14**:8965 (2024). https://doi.org/10.1038/s41598-024-58970-3.

72 Ritchie H, How will climate change affect crop yields in the future? Our World in Data https://ourworldindata.org/will-climate-change-affect-crop-yields-future [accessed 12 February 2025].

73 Fick SE and Hijmans RJ, WorldClim 2: new 1-km spatial resolution climate surfaces for global land areas. *Int J Climatol* **37**:4302–4315 (2017). https://doi.org/10.1002/joc.5086.

74 Karger DN, Conrad O, Böhner J, Kawohl T, Kreft H, Soria-Auza RW *et al*., Climatologies at high resolution for the earth's land surface areas. *Sci Data* **4**:170122 (2017). https://doi.org/10.1038/sdata.2017.122.

75 FAO, *Establishing a National Plant Protection Organization: A Guide to Understand the Principal Requirements for Establishing an Organization to Protect National Plant Resources from Pests*. Food and Agriculture Organization of the United Nations, Rome, Italy (2015).

76 Kfir R, Overholt WA, Khan ZR and Polaszek A, Biology and management of economically important lepidopteran cereal stem borers in Africa. *Annu Rev Entomol* **47**:701–731 (2002). https://doi.org/10.1146/annurev.ento.47.091201.145254.